Negative Electric Vehicle Emissions: Vehicle-to-Grid Incentivizes Enough Wind and Solar Investment to Reverse EV Charging Emissions

Jiahui Chen[a,b], Michael T. Craig[a,c], Jeremy Michalek **[b,d,e], Matthew Bruchon[b], Parth Vaishnav[a]

[a]*School for Environment and Sustainability, University of Michigan, Ann Arbor, MI 48109, USA*

[b]*Department of Engineering and Public Policy, Carnegie Mellon University, Pittsburgh, PA 15213, USA*

[c]*Department of Industrial and Operations Engineering, University of Michigan, Ann Arbor, MI 48109, USA*

[d]*Department of Mechanical Engineering, Carnegie Mellon University, Pittsburgh, PA 15213, USA*

[e]*Department of Civil and Environmental Engineering, Carnegie Mellon University, Pittsburgh, PA 15213, USA*

Abstract

Consequential emissions analyses of power system interventions typically overlook induced structural changes. We estimate the consequential power system emission effects of plug-in electric vehicle (PEV) charging due to both operational effects and induced renewable investments. We study PJM, the largest U.S. grid operator, with a grid mix representative of North America, assuming 10% fleet electrification. Immediate post-trip charging raises grid emission externalities by increasing fossil fuel generation and provides little renewable investment incentives. However, flexible, cost-minimizing charging creates economic incentives to increase wind and solar capacity investment by 4.4%. The effect increases to 23% with bidirectional vehicle-to-grid (V2G). This induced investment reverses PEVs' emission effects: estimates ignoring capacity changes show PEVs increase grid emissions externalities by $240–610 per PEV-year, whereas estimates accounting for induced renewable investments show *adding* PEVs *reduces* grid emission externalities by $230 per PEV-year with flexible charging and $2200 per PEV-year with V2G.

Keywords: Electric vehicles , Energy storage, Renewable energy, Climate change, Externalities

Email address: jmichalek@cmu.edu (Jeremy Michalek **)

1. Introduction

The rapid adoption of plug-in electric vehicles (PEV) and the wide deployment of wind and solar power are at the center of climate actions of many major economies. Global PEV sales in 2023 exceeded 14 million, accounting for 15.8% of all new car sales, up from 2.6% in 2019 and 5% in 2020 [1]. With the steady decline of PEV costs and commitment to current and future PEV incentive policies, PEV sales will likely continue to grow in the coming decades [1, 2]. Deployment of wind and solar power (referred to as WSP in short) has also grown significantly in recent years due to falling costs and policy support aimed at reducing power sector emissions [3, 4]. In the U.S., wind and solar supplied 14% of all electricity demand in 2022, up from 2% in 2010.

While expanding PEV fleets and growing wind and solar capacity are critical to mitigating climate change, they also make it more challenging to reliably balance electricity supply and demand [5–7]. Additionally, increasing wind and solar penetration can suppress electricity prices and thus reduce electricity revenues for generators, which could make it uneconomical to reach high levels of wind and solar penetration [8–10]. To overcome these challenges, load flexibility could be helpful. PEVs have the potential to provide load flexibility through cost-minimizing PEV charging and bidirectional vehicle-to-grid (V2G) technology [11–15], and this potential could substantially affect the power system emissions implications of growing PEV load.

Past studies estimating the consequential effect of PEV charging on power systems typically capture the effect of PEV load on power system operations while assuming the generation infrastructure is exogenous and unaffected by PEV load, as shown in Table 1's left column [16–28]. Gagnon et al. [29] and Holland et al. [30] argue that this short-run approach is misleading because it misses the potential for load increase to induce new wind and solar construction, fundamentally affecting the long term potential benefits of the transition to PEVs. To date, the few studies that have attempted to estimate the effect of PEV load on generator capacity have all used simplified or non-representative load profiles (which can have different implications for incentivizing wind and solar construction) and/or have excluded cases with cost-minimizing charging or vehicle to grid, as shown in Table 1's right column [31–39] (a more detailed breakdown of this literature is provided in the Supplemental Information).

We bridge this gap by developing a model to estimate how power system generation capacity is endogenously affected by PEV load, cost-minimizing charging, and vehicle to grid (addressing the bottom-right corner of Table 1). We leverage a power systems optimization model of the PJM Interconnection – the largest regional transmission organization in the United States serving 65 million people across 13 states and the District of Columbia with a grid mix similar to North America as a whole [7, 19, 20, 40]. Based on PJM's Interconnection queue and capacity expansion study, we model the generation fleet with different wind and solar capacity levels. We simulate grid operations both with and without added PEV loads across these wind and solar capacity levels, and we identify maximum economical wind and solar capacity levels under each PEV load scenario.

We find that, with uncontrolled charging, transitioning 10% of the vehicle fleet to PEVs increases power grid greenhouse gas and air pollutant emission externalities by $330 per PEV in 2035 (1.59 tons of CO_2 per vehicle or 1% of overall power system externalities) by increasing generation from existing fossil fuel generators, compared with a no PEV base case. Uncontrolled charging

Table 1: Contribution to the literature: We estimate effects of PEV load on power system generator capacity using realistic BEV load profiles, cost-minimizing charging and V2G scenarios

		Effect of PEV load on power system generator capacity	
		Ignored	Included
Realistic high-resolution BEV charging profiles with V1G and/or V2G	No	[21, 23, 24, 27, 41]	[31–39, 42, 43]
	Yes	[7, 16–20]	**This paper**

minimally increases investment in wind and solar capacity (only 300 MW increase). When capacity expansion is ignored, charging with cost-minimizing charging and V2G increases these emission externalities by $240 and $610 per PEV, or 1.03 tons and 2.34 tons of CO_2 per vehicle, respectively, compared with a no PEV base case. However, when capacity expansion is modeled, cost-minimizing charging and V2G reduce power system air emission externalities by $230 and $2200 per PEV, respectively, compared to a no PEV base case. This is achieved by increasing the cost-effective levels of wind and solar capacity by 4.3% and 23%, compared to a no PEV base case. The potential for PEV charging to trigger infrastructure investment that reduces emissions implications is consistent with[30] and [37], and our study finds that flexible charge timing and especially V2G can make this effect large enough to flip the direction of PEV charging effects on power system emissions. Thus the ability of flexible PEV load to incentivize new wind and solar construction produces the result that adding additional demand for electricity can result in a net reduction in power system emissions.

2. Results

We model PEVs with three kinds of charging behaviors: uncontrolled charging (UC), cost-minimizing charging (CC), and vehicle-to-grid (V2G). In uncontrolled charging, vehicles are fully charged as soon as plugged in at home at the end of the day. In cost-minimizing charging, charging is co-optimized with power system dispatch within constraints, such as requiring the vehicle to be fully charged before morning departure. In V2G, charging and discharging back to the grid is co-optimized with power system dispatch, within constraints. A more detailed description is provided in Section 4.1 and Section 4.2 in the Materials and Methods section.

2.1. Wind and solar capacity investment induced by PEV charging

To capture the long-run effects of PEV charging on the power system, we calculate the maximum profitable wind and solar installation under each charging intervention scenario. Annual hourly power system operation is simulated to acquire short-term revenue results for wind and solar under a range of wind and solar capacity scenarios. The aggregate revenues are then compared with the aggregate annualized fixed cost associated the installed capacity. We define the maximum profitable capacity as the highest capacity for which revenue exceeds annualized fixed costs (variable generation costs are considered negligible for wind and solar). Aggregated results for wind and solar generators are depicted in Figure 1. When aggregated wind and solar revenues equal total fixed costs (labeled intersection points in Figure 1), capacity achieves its maximum profitable level.

In a baseline PJM system without PEVs, we estimate combined solar and wind capacity could reach 63.9 GW while maintaining profitability (Figure 1) assuming moderate projected wind and solar fixed cost through 2035 (55.9 to 70.8 GW at low and high projected wind and solar costs). Projected costs used to assess annualized fixed costs for wind and solar power are described in method Section 4.5. Installed wind and solar capacity in PJM as of the end of 2023 totalled 22 GW, and 143 GW sit in the interconnection queue, indicating ample interest in further wind and solar deployment [44]. Converting 10% of vehicles to PEVs in PJM can significantly increase the maximum profitable capacity of wind and solar, depending on the charging strategy used. With uncontrolled charging, the maximum profitable capacity of wind and solar increases by only 300 MW, indicating PEV deployment with uncontrolled charging only induces negligible investment in wind or solar power. But with cost-minimizing charging, the maximum profitable capacity of wind and solar increases by 2.8 GW (a 4.4% increase) bringing the total combined wind and solar capacity to 67 GW. With V2G, the maximum profitable capacity of wind and solar capacity increase by 15 GW (a 23% increase), bringing the total capacity to 80 GW.

Uncontrolled PEV charging tends to add load when wind and solar generation is low, yielding little induced capacity investment. Conversely, cost-minimizing charging of PEVs allows PEV load to be shifted to periods with low net demand, when wind and solar generation is high. Cost-minimizing charging thus reduces wind and solar curtailment and increases electricity prices in these hours, increasing revenues and making a higher level of wind and solar capacity investment profitable. In addition to charge timing flexibility, V2G also provides storage services, resulting in larger benefits for wind and solar revenue and inducing greater investment.

2.2. Electricity generation induced by PEV charging

PEV charging affects power system electricity generation directly by increasing demand or, in the case of V2G, providing electricity storage to the grid, and it also affects generation indirectly through induced investment in wind and solar capacity (Figure 2). Here, we separate these two factors by comparing two sets of scenarios that (1) ignore or (2) capture induced wind and solar investment by PEVs. Within each set of scenarios, we quantify the effect of PEVs on electricity generation by comparing scenarios with PEVs and different charging strategies to a reference scenario without PEVs.

When we ignore induced wind and solar capacity investment, PEVs with uncontrolled charging increase combined cycle natural gas generation by 6.4 TWh relative to the NoPEV case, or 1.1 MWh per MWh of PEV charging. As the uncontrolled charging demand roughly coincides with the daily load peaks, when renewable generation is low, PEV load is met with combined cycle natural gas generators. Little curtailment of wind and solar occurs (0.5% of total generation), and uncontrolled charging does not align with curtailed renewables, so it does not mitigate curtailment. Cost-minimizing charging and V2G provide additional flexibility demand timing, allowing the system to use otherwise curtailed renewables. Due to low wind and solar curtailment rates, cost-minimizing charging only increases wind and solar generation by 0.18 MWh per MWh of PEV charging. Instead, cost-minimizing charging increases low-marginal-cost coal generation by 1.2 MWh, combined cycle natural gas generation by 2.0 MWh, and nuclear generation by 0.17 MWh per MWh of PEV charging. Demand flexibility enabled by cost-minimizing charging also leads to a 2.5 MWh reduction in high-marginal-cost gas turbine natural gas generation per MWh of PEV charging. Similar changes occur with V2G charging. V2G only increases wind and solar

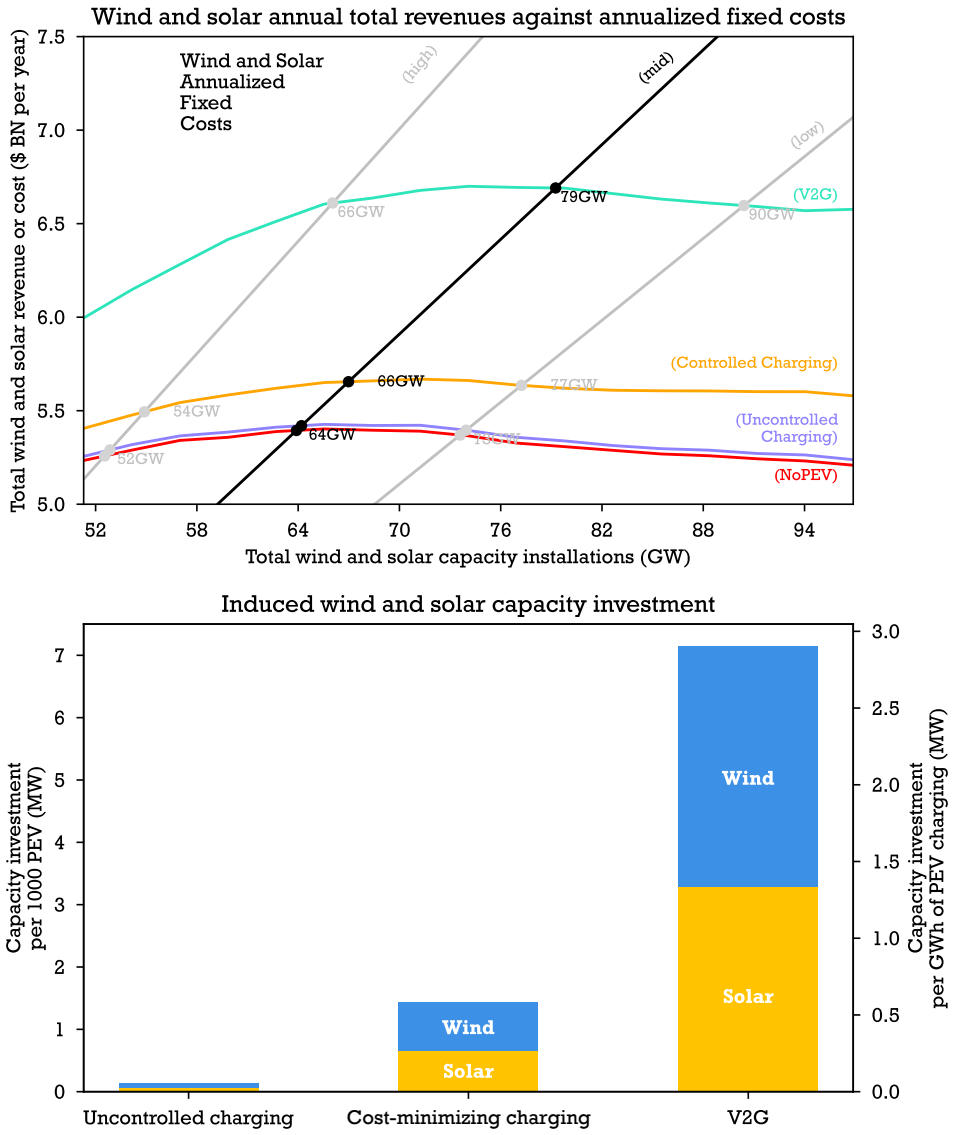


Figure 1: Effect of PEV charging load on the economics of wind and solar capacity investment. Top panel: Total revenues and total annualized fixed costs for solar and wind generators, by PEV and PEV charging intervention scenarios and by wind and solar fixed cost scenarios. (high): conservative fixed cost scenario, (mid): base case fixed cost scenario, (low): optimistic fixed cost scenario. Wind and solar are modeled together at a fixed ratio, as described in the Method section. For each cost case we find the intersection of the annualized total fixed cost curve and the revenue curve, the intersection represents the maximum profitable total wind and solar capacity. Beyond this point additional wind or solar capacity cannot be added profitably. Bottom panel: Wind and solar capacity investment induced by PEV charging interventions, including uncontrolled charging (UC), cost-minimizing charging (CC) and vehicle-to-grid (V2G), relative to the NoPEV baseline scenario. Changes of the maximum profitable wind and solar capacity compared to the NoPEV baseline scenario are considered capacity investment induced by PEV and PEV charging interventions. The currency unit is 2024 USD. $ BN is short for billion USD. Further detailed methods are described in method Section 4.3.

generation by 0.50 MWh and nuclear generation by 0.46 MWh per MWh of PEV charging, while

increasing coal generation by 3.6 MWh, combined cycle natural gas generation by 0.84 MWh. Gas turbine natural gas generation is reduced by 4.4 MWh per MWh of PEV charging.

When we account for induced wind and solar capacity expansion, the effect of PEVs on the generation mix changes substantially under cost-minimizing charging and V2G scenarios but not under the uncontrolled charging scenario. Uncontrolled charging does not induce significant wind and solar capacity investment (0.2 GW, Figure 1), so generation mix changes are the same when accounting for or ignoring induced wind and solar capacity investment. But cost-minimizing charging and V2G scenarios do induce wind and solar investment, resulting in increasing wind and solar generation that displaces coal- and gas-fired generation. With cost-minimizing charging, additional flexibility increases wind and solar generation by 1.3 MWh per MWh of PEV charging, coal generation by 0.80 MWh, and combined cycle natural gas generation by 1.4 MWh. Gas turbine generation is reduced by 2.4 MWh per MWh of PEV charging. With V2G, additional flexibility increases wind and solar generation by 7.7 MWh per MWh of PEV charging, and coal generation by 1.2 MWh. Gas turbine generation is reduced by 4.4 MWh, and combined cycle natural gas by 3.3 MWh per MWh of PEV driving.

As a result of generation mix changes, total system costs differ under different charging scenarios. When ignoring induced wind and solar capacity investment, total system costs under V2G are 6% lower than without PEVs (a $400 per PEV per year reduction). When accounting for induced wind and solar capacity investment, total system costs under V2G are 13.4% lower than without PEVs (an $880 per PEV per year reduction).

2.3. Air emission externalities induced by PEV charging

PEV charging affects power system greenhouse gas (GHG) and local air pollutant emissions through its effect on induced capacity investment and electricity generation (Figure 3). We estimate externality costs of these emissions using a $204 per mt CO_2eq social cost of carbon [45] and using the AP3 model for estimating air pollution-related mortality risk with a $8.7M value of reduced mortality risk [46].

When we ignore induced wind and solar capacity investment, PEV charging increases emissions externalities by increasing fossil-fuel generation (Figure 2). As shown in Figure 3 PEV adoption increases overall 2035 power system air emission externalities by $330, $240 or $610 per PEV when charging is uncontrolled, cost-minimizing, or V2G, respectively.

When we account for induced wind and solar capacity investment, uncontrolled PEV charging still increases power system air emission externalities by $330 per PEV, as before, but because cost-minimizing charging and V2G induce new wind and solar capacity investment, PEV charging *reduces* total power system air emission externalities by $230 or $2200 per PEV for cost-minimizing charging and V2G, respectively.

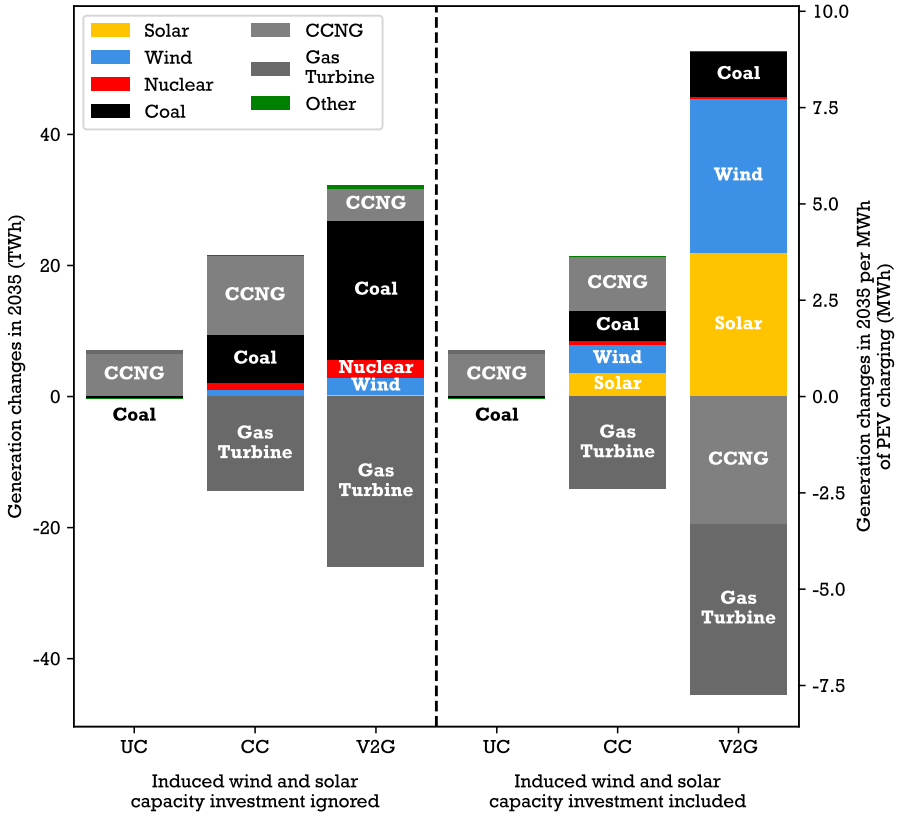


Figure 2: Effect of PEV charging load on power generation. Changes in annual generation by fuel type, relative to the NoPEV case, for each PEV charging scenario when ignoring versus including induced wind and solar capacity investment. When accounting for induced wind and solar investment, Wind and solar capacity and therefore generation vary across PEV charging scenarios. 'UC': uncontrolled charging; 'CC': cost-minimizing charging; 'V2G': vehicle-to-grid. 'CCNG' fuel type includes combined cycle natural gas generators. 'Other' fuel types include biomass, fossil waste, fuel cell, hydro, landfill gas, municipal solid waste, non-fossil waste, and oil or gas steam.

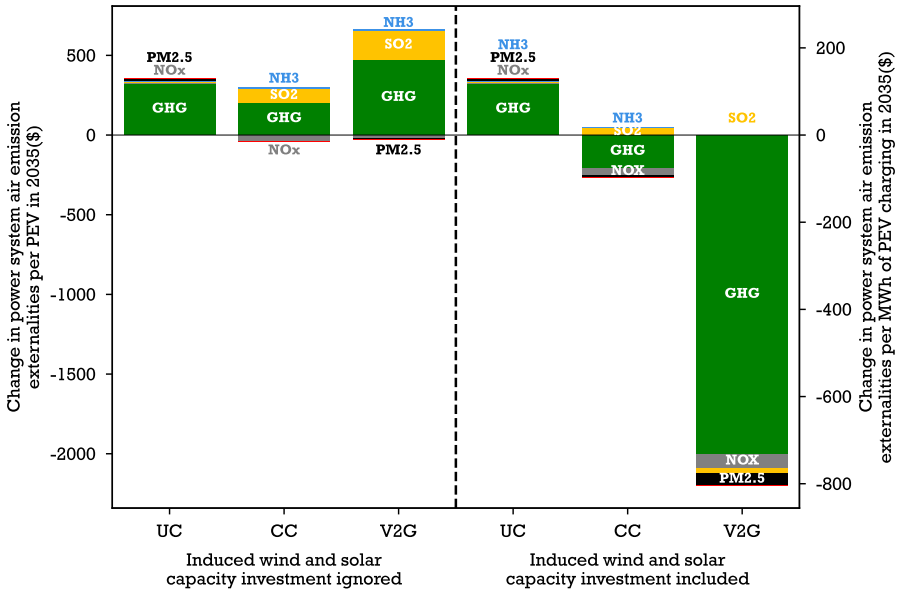


Figure 3: Effect of PEV charging on power system air emission externalities. Change in total power system air emission externalities per PEV and per MWh of PEV charging in 2035, relative to the NoPEV scenario, under each PEV charging scenario when ignoring versus including induced wind and solar capacity investment. The 'ignored' scenarios use generation portfolios given by PJM's grid planning study for 2035 [47]. The 'included' scenarios consider wind and solar capacity at maximum profitable capacity, as described in Method and Materials. 'GHG' is short for greenhouse gases. When induced wind and solar capacity investment is ignored, PEV load increases power system air emission externalities. When it is included, uncontrolled PEV load increases power system air emission externalities, but cost-minimizing charging (CC) and vehicle-to-grid (V2G) scenarios induce enough wind and solar capacity investment to produce a net reduction in power system air emission externalities.

2.4. Sensitivity analysis

Under all sensitivity scenarios, V2G benefits persist in 1) inducing wind and solar capacity investment; 2) system cost reduction; and 3) power system emission externality reduction (shown in Table 2). However, substantial variations exist depending on the tested parameters. Detailed results for each sensitivity scenario are in the SI.

Changing from the base case to the high renewable fixed cost scenario led to a 10% decrease in induced investment in wind and solar capacity per PEV, a 3.6% decrease in system cost reduction per PEV, and a 15% decrease in emission externality reduction per PEV. Changing from the base case to the low renewable fixed cost scenario led to a 9.9% increase in induced investment in wind and solar capacity per PEV, a 0.22% decrease in system cost reduction per PEV, and a 15% decrease in emission externality reduction per PEV. Though fixed costs vary substantially across the three scenarios, V2G contribution to system cost reductions and emission externality reductions are substantial, indicating the robustness of results against fixed cost levels. Meanwhile, since the real discount rate assumed by the model also determines fixed costs, the fixed cost sensitivity results also indicate the robustness of results against real discount rate.

Increasing stationary storage capacity from 5.4 GW (42 GWh) to 14 GW (56 GWh) led to a 74% decrease in induced investment in wind and solar capacity per PEV, an 80% decrease in system cost reduction per PEV, and a 71% decrease in emission externality reduction per PEV. The significant dilution of the V2G value in a power system with high stationary storage capacity suggests the substitution of stationary storage by V2G.

Doubling transmission storage capacity led to a 21% increase in induced investment in wind and solar capacity per PEV, a 25% increase in system cost reduction per PEV, and a 32% increase in emission externality reduction per PEV. The significant enhancement of V2G value in a power system with high transmission capacity suggests synergies between transmission capacity expansion and V2G.

Increasing PEV fleet penetration from 10% to 20% resulted in a 15% decrease in induced investment in wind and solar capacity per PEV, a 19% decrease in system cost reduction per PEV, and a 32% decrease in emission externality reduction per PEV. Despite doubling PEV penetration, the contribution per PEV to cost savings and emission reductions was not severely diluted, highlighting the scalability of PEV integration.

Adjusting the wind-to-solar capacity ratio from 1.17 to 1.43 led to a 4% increase in induced investment in wind and solar capacity per PEV, a 14% increase in system cost reduction per PEV, and a 4% increase in emission externality reduction per PEV. Adjusting the wind-to-solar capacity ratio from 1.17 to 0.96 led to a 20% increase in induced investment in wind and solar capacity per PEV, a 14% increase in system cost reduction per PEV, and a 4.5% increase in emission externality reduction per PEV. The higher performance of V2G under the high solar scenario could be attributed to the relatively low costs of solar PV compared to wind.

The sensitivity analysis shows variations in system cost reduction and emission externality reduction across different parameter settings. However, the value of V2G remains positive in all cases, demonstrating its potential to deliver consistent benefits across a variety of system conditions.

Table 2: Sensitivity Analysis: Robustness of V2G Results to Parameter Variations.
Estimates are relative to the base case V2G effect estimates.

Input parameters	Baseline value	Tested value	Induced wind and solar capacity investment per PEV	Annual system cost reduction per PEV per year	Annual emissions externality reduction per PEV	Interpretation
Stationary storage capacity	5.4 GW 42 GWh	14 GW 56 GWh	-74%	-80%	-71%	PEV V2G has smaller (but positive) benefits for power systems with more stationary storage.
Transmission capacity	Varies	2× baseline	+21%	+25%	+32%	PEV V2G has larger benefits in power systems with more transmission capacity.
PEV fleet penetration	10%	20%	-15%	-19%	-32%	Larger PEV fleets yield diminishing returns.
Wind to solar capacity ratio	1.17	1.43 0.96	+4% +20%	+14% +14%	+4% +4.5%	PEV V2G benefits vary with assumed wind-to-solar ratio.

3. Discussion and Limitations

3.1. Limitations and caveats

Our estimates are based on optimal grid operations and optimal use of PEV charging flexibility. In practice, benefits may be somewhat lower because of limitations in the ability to forecast load, variable renewable generation, and PEV availability, and to coordinate charging decisions among millions of PEV households.

We acknowledge that V2G may potentially change battery degradation, and device/infrastructure upgrades could be required for V2G. If such costs are accounted for during V2G operation, there will be fewer energy arbitrage opportunities for V2G. As a result, V2G could produce lower cost reductions and emission reduction benefits. However, some studies have suggested Li-ion batteries are very durable to cycling, and additional battery cycling from V2G may not be problematic [48–54].

We treat wind and solar together assuming a fixed 54% to 46% capacity ratio based on the mix of wind and solar resources in the interconnection queue. Moreover, we assume future wind and solar capacity expansion will follow the current geographical distribution. Actual wind and solar build-outs may be more strategic, adding uncertainty to our estimates. For example, optimal wind and solar development may result in less curtailment than under a fixed ratio assumption. Hence flexible loads and storage provided by cost-minimizing charging and V2G would render less valuable. We run sensitivity analyses with high wind capacity and high solar capacity respectively. In the high wind case, V2G's cost reduction is 14% higher than under the base case, and the emission externality reduction is 4.0% higher. In the high solar case, V2G's cost reduction is 14% higher than under the base case, and the emission externality reduction is 4.5% higher. The analysis reveals variability in the magnitude of results; however, the value of V2G remains positive and substantial under all tested conditions, reinforcing its potential to deliver economic and environmental benefits. More details are provided in the SI.

Our estimated benefits are based on wind and solar investment decisions driven by economic viability. Other factors, such as national, state, and local regulations, incentives, process delays, or political factors may also influence realized investment decisions in practice. For example, wind and solar PV projects make up 93% of PJM's interconnection queue, but a growing backlog of new wind and solar project requests indicates the interest in investment is not matched by the actual build-out[55]. Furthermore, we analyze a state of long-run equilibrium, where all profitable wind and solar generators are built, representing long-run perfect competition where free entry and exit result in implementation of all profitable construction (in contrast to single firm profit maximization, where marginal cost equals marginal revenue). In doing so we ignore the time lag between market, investment, and the actual buildout, and we ignore other deviations from perfect competition outcomes. For simplicity, data availability, and computational reasons, we also assume that generation profiles and expansion costs are identical across all wind and across all solar generators, regardless of location. Location-resolved values could improve upon our estimates.

Our power system model accounts for planned capacity changes in the generator fleet covered in EIA Form 860 and projected in PJM's 2021 Energy Transition study, but we do not consider the potential impacts of future policies on the power system [47]. As a result, coal-burning generation

capacity in this study may differ from the real world, depending on the policy environment. We assume the same coal power plant capacity to match the projected coal capacity in the 'Accelerated' scenario of PJM's 2021 Energy Transition study [47]. However, state and federal regulations such as the Revised Clean Air Act Section 111(d) could eliminate coal power plants by 2035, and other changes in policy could accelerate or delay coal retirement.

We do not model transmission capacity expansion endogenously, but we run a sensitivity analysis with double the transmission capacity of the base case to investigate this uncertainty. In the high transmission cases, V2G yields 25% more system cost reduction and 32% more emission reduction compared with the base case. This indicates synergies instead of competition exist between transmission capacity expansion and V2G. More details are provided in the SI.

We only model flexible loads from PEVs and none from other sources. Other flexible loads and increases in PEV fleet size may dilute the benefits of PEV cost-minimizing charging and V2G. We run a sensitivity analysis where 8.4 GW stationary storage is added to the system and a case with a PEV penetration of 20% instead of 10% in the base case. In the high storage case, the cost reduction and emission externality reduction benefits per PEV are reduced by 80% and 71%. In operation, V2G provides energy storage services, filling the same role as utility-scale storage units. In the high PEV penetration case, the cost reduction and emission externality reduction benefits per PEV are only reduced by 19% and 32% respectively. More details are provided in the SI.

We note that alternative "uncontrolled" charging schedules, such as daytime charging rather than charging after the last trip of the day, could potentially create different incentives for wind and solar capacity investment, which could also affect consequential emissions of PEV charging without cost-minimizing charging [39].

3.2. Discussion

We find that a 10% increase in PJM PEV adoption does not induce additional wind and solar capacity investment when each vehicle is charged (uncontrolled) after the last trip of the day. But when PEV charge timing is scheduled to minimize cost, and especially when PEVs have bidirectional V2G capabilities, adding PEV load can increase profitable levels of wind and solar capacity investment so much that net power system air emissions externality costs actually drop.

Our estimates suggest that the adoption of cost-minimizing charging or V2G reduces the power system air emission externality cost consequences of PEV adoption by $230 and $2200 per PEV per year, respectively, in 2035 PJM, suggesting a policy rationale for incentivizing adoption of cost-minimizing charging and V2G. Our estimates also suggest that consequential life cycle air emissions externalities of PEV adoption may be smaller than estimated in prior studies [20] if the PEVs use cost-minimizing charging or V2G.

Home chargers capable of receiving signals from a utility and adjusting the timing and rate of charging in response are needed to enable cost-minimizing charging. For V2G, this term sometimes implies bidirectional flow to and from the power grid, which requires special grid connections typically unavailable at the household level. But the term V2G sometimes implies only bidirectional flow from the vehicle to the home to displace household load without requiring a bidirectional connection between the home and the power grid (also known as vehicle-to-home).

Our analysis is agnostic to these V2G variations so long as household load exceeds vehicle discharge in the analysis. However, the V2G cases that we model implicitly assume bidirectional communication between the vehicle and the power grid, which is needed to determine whether PEVs are plugged in and how much headroom PEV batteries have to charge or discharge at a given moment. The development of such communication systems and algorithms to aggregate information and distribute control would be necessary to realize large V2G adoption of the type modeled here.

We use the term "long-run consequential emissions" for our estimates and avoid the term "long-run marginal emissions" used in [29] because marginal emissions are a special case of consequential emissions for which the change in question is a single unit (for discrete quantities or the derivative for continuous quantities) [56]. Our study involves a 10% change in PEV adoption, which is too large to be considered marginal.

We focus on PEV charging load, but other kinds of grid interventions with flexible loads also have the potential to induce wind and solar capacity investment. For example, building electrification with the deployment of air source heat pumps can increase grid emissions due to additional load [57–59]; however, combined with load control, the additional load can incentivize solar and wind investment, which serves not only the heat pump load but also the rest of the power system, thus helping to facilitate the decarbonization of the whole power system. To harness the discussed benefits, it is suggested that power system operators and energy management service providers actively explore both the technical and economic viability and market designs for potential grid flexibility solutions. With mature business models, these grid flexibility solutions may help the power system reduce both costs and emissions in its transition to carbon neutrality.

4. Materials and Methods

This study develops an approach to assess emission effects of grid intervention technologies in both power system operation and in power system structural changes. The analysis is based on a short-term power system operational cost model that has an embedded PEV behavioral module. The short-term model allows highly resolved representation of real-world PEV operational constraints. Then short-term operational results are translated to long-term capacity expansion decisions and thus inform long-term structural changes of the power system. In the end, emission changes in greenhouse gases (GHG) and local air pollutants are assessed considering the induced capacity expansion. As a case study, we analyze a 2035 version of the PJM Interconnection under three grid interventions: PEVs with uncontrolled charging, cost-minimizing charging, and vehicle-to-grid (V2G).

4.1. PEV behavioral model

As we use a short-term operational cost model to simulate power system operation, we are allowed higher granularity when it comes to mathematical abstraction of PEV operational constraints[41, 60]. We model an electric light-duty vehicle (LDV) fleet that takes up 10% of the LDV fleet in PJM. This PEV stock penetration is plausible, as PEV penetration in new light-duty vehicle sales is expected to reach 11% in 2024 in the US, and the US market is expected to grow [1]. To test result robustness, we also run sensitivity analyses with 20% PEV penetration. As computational

power is limited, a simplifying assumption is made that the PEV fleet is made up of generic battery electric vehicles with a 300 mile (480 km) range.

We model three kinds of charging behaviors: uncontrolled charging, cost-minimizing charging, and vehicle-to-grid (V2G). When the electric vehicle charging is uncontrolled, the PEVs engage in convenience charging, meaning PEVs fully charge their battery at the maximum available charging rate at the end of each day at home. Under cost-minimizing charging, the PEVs are always plugged in and can be charged when parked. The charging schedule is co-optimized with the power system economic dispatch during the hours that the PEV is parked and plugged in and within battery capacity constraints. PEVs are required to be fully recharged before the first trip of the following day to be ready for travel. The third charging behavior is V2G. Under V2G, PEVs are always plugged in when parked and can participate in V2G. PEVs that participate in V2G can release energy to or draw energy from the power grid, within operating constraints, allowing charging rates to be negative. The detailed model representation of these operational constraints is described in SI.

In order to represent PEV energy consumption and charging availability across the fleet, we use 15 weighted daily vehicle travel profiles from the National Household Travel Survey (NHTS) to represent 15 groups of PEVs with distinct driving profiles selected to mimic the behavior of the overall fleet as closely as possible, as described in Weis et al. 2014 [34]. These daily driving profiles include the time of the first trip and the last trip of the day, hourly plugged-in availability, and hourly vehicle miles traveled of each hour of the day. The hourly plugged-in availability describes the proportion of PEVs in each PEV behavioral group that are parked and available for charging. Each PEV group has its distinctive driving behavioral pattern. Besides PEVs that are driven, we also model PEVs that are not driven on that day. The NHTS data indicates 30% of vehicles whose owners were surveyed are not active and do not have travel records on the day of survey. Hence, we also a group of PEVs that do not have driving events for the day. For simplicity and due to data limitations, energy consumption profiles and availability profiles are assumed to be the same every day throughout the year for each group, and driving behavioral patterns are assumed to be homogeneous within each group. The total numbers of PEVs in each region of PJM is calculated as proportional to the region's population. We compared the 2009 NHTS dataset and the 2017 dataset and found that daily vehicle miles traveled per household did not change significantly, and thus we adopt the 2009 analysis used in [34].

4.2. Power system model

We run a unit commitment and economic dispatch (UCED) model to simulate the day-ahead energy market and reserve requirements of the PJM Interconnection. This model was first developed by Lueken et al. [40] and later adapted by Weis et al. [7, 19] to incorporate electric vehicle battery charge tracking. The UCED model minimizes variable costs of generators including variable operation and maintenance costs, startup costs, and fuel costs in sliding 48-hour optimizing windows. After solving each window, the model accepts the results of the first 24 hours and moves forward by 24 hours until a full year's optimization is completed. Our UCED models the PJM Interconnection as 5 transmission-constrained regions, inside each of which there is assumed to be no transmission losses or constraints. In each region, energy demand is constrained to be equal to supply at every time step, and reserve requirements must be met. Operational characteristics

of dispatchable generating units, including ramp rates, minimum uptime, and minimum downtime, are modeled through sets of constraints. The operation of solar and wind generators is also modeled, where excessive wind and solar generation can be curtailed when needed.

We incorporate each PEV charging scenario into the UCED model. PEV uncontrolled charging load is added to the baseload, as it is inflexible. PEVs with cost-minimizing charging and V2G are modeled similarly to storage units with limited availability: charging and discharging are limited by the hourly availability of PEVs that are plugged in, and they need to be fully charged before the first trip of the following day. As discussed in method Section 4.1, 30% of PEVs do not have driving events on any given day. We model this group of PEVs as stationary storage with the same power capacity and energy capacity. During the day, energy depletion from driving is modeled as energy drawn from batteries, realized through extra sets of constraints that track PEV battery states of charge and regulate their charging and discharging rates. The detailed model formulation can be found in the SI.

4.3. Power system scenarios and data sources

Given expected wind and solar capacity growth in PJM's near-term plans and the fact that wind and solar account for most of PJM's interconnection queue [47, 61], we model a 2035 PJM power system by increasing wind and solar installed capacity from the current PJM system. We use a PJM system dataset that was first compiled by Weis et al. 2016 and updated by Bruchon et al. 2024 [7, 20]. This dataset includes operational characteristics of dispatchable generators, including heat rate, capacity, location, variable operation and maintenance costs, ramp rates, minimum up and down time, startup cost, and minimum load from the U.S. Energy Information Administration (EIA) Form 860, the National Electric Energy Data System (NEEDS) dataset from 2020, and other data sources described in Weis et al. 2016 [7, 62, 63]. Retirement and new installations of dispatchable generators (mainly fossil fuel generators) are based on planned generator retirements and installations through the scenario year 2035 [20, 62]. We assume the same coal power plant capacity as the projected coal capacity in the 'Accelerated' scenario of PJM's 2021 Energy Transition study[47]. The baseline wind and solar penetration as a percentage of total demand is 22%, based on the 'Policy' scenario of the study. Since we analyze beyond the wind and solar penetration of the 'Policy' scenario and investigate further decarbonization, we used the 'Accelerated' scenario for coal capacity. We first implement all retirement scheduled by Form 860, and retire the remaining coal power plants, from the plants with the oldest NEEDS online years, until the total capacity matches the capacity assumed in the PJM study. The total capacity of dispatchable generators excluding hydro electric generators is 170 GW. This dataset models existing storage units based on 2020 EIA Form 860 and storage capacity expansion based on PJM's energy transition study [47, 62]. Combining pumped hydro storage and battery storage, PJM is assumed to have 5.4 GW (42 GWh) grid-scale storage units. PJM's DataMiner provides 2020 hourly wind and solar generation profiles, load profiles, and transfer limits across PJM [64]. Fuel prices for each fuel type are retrieved from 2019 EIA Form 923 data[65].

PJM's recent energy transition and grid planning study models a 'Policy' Scenario where wind and solar supply 22% of total electricity consumption by 2035 with stated policies, and an 'Accelerated' Scenario where wind and solar supply 50% of total electricity consumption by 2035[47]. Active solar PV and wind projects in PJM's interconnection queue reached 207 and 103 GW, respectively, as of June 2024, indicating mounting interest in wind and solar development [61]. Based on

PJM's 'Policy' and 'Accelerated' Scenarios and the PJM Interconnection queue, we create 25 high wind and solar penetration scenarios that increase wind and solar generation from 22% to 46% of electricity consumption (excluding PEV and assuming no curtailment) in 1% increments. Solar and wind capacities in our generator fleets range from 24 to 56 GW and 27 to 66 GW, respectively. To estimate hourly wind and solar generation for each of our 25 scenarios, we combine historic wind and solar output and installed capacity with wind and solar capacity expansion projections from PJM[47, 64]. First, we spatially aggregate 2020 historic observed generation and capacity of solar PV and onshore wind from 20 control zones in PJM to our five regions[64]. For each of our five regions, we use generation and capacity to calculate hourly capacity factors for solar PV and wind by region. We assume the same capacity factors for onshore and offshore wind given a lack of historic generation data for offshore wind. Offshore wind only accounts for up to 15% of wind and solar capacity in our scenarios.

To scale up wind and solar capacity to create each of our 25 scenarios, we assume the capacity ratio of future wind and solar project types will remain the same as projected in PJM's energy transition study[47]. First, we use PJM interconnection queue to determine how the capacity expansion is distributed across regions for wind and solar, i.e. what percentage of wind and solar is installed in each of the 5 regions [64]. The ratio of capacity installation of solar to wind for the whole PJM is determined using the PJM energy transition study [47], i.e. what is the ratio of solar capacity installation to wind capacity installation for the whole PJM. With this fixed ratio of wind and solar capacity, we scale up both two capacities until total wind and solar generation, calculated as regional capacity times regional capacity factor by generator type, equals the desired combined wind and solar penetration. This method may overestimate future wind or solar capacity factors given that higher resource sites are likely to have already been developed, but efficiency gains in wind and solar technology will at least partly counteract this effect.

We run annual UCED simulations for all pairwise combinations of our 25 wind and solar scenarios and 4 PEV charging scenarios (no PEVs and PEVs with uncontrolled charging, cost-minimizing charging, and V2G, described in method Section 4.1), yielding 100 UCED simulations that allow us to quantify PEV impacts at varying wind and solar penetration levels and charging approaches.

4.4. Air emission externality costs

We quantify operational stage power system greenhouse gas (GHG) and local air pollutant emissions and estimate consequent air emission externality costs. Emission factors of GHGs and local air pollutants for each generator are retrieved from the National Emissions Inventory (NEI) [66]. For generators that cannot be found in NEI, we substitute with the average emission factor in NEI based on the fuel type. To estimate air emission externality costs, we use a social cost of carbon of \$204/ton CO_2e [45] for GHGs. For local air pollutants, we assess emissions of sulfur dioxide (SO_2), nitrogen oxides (NO_X), ammonia (NH_3), fine particulate matter ($PM_{2.5}$), and volatile organic compounds (VOCs). Externality costs from local emissions are calculated on a spatially-explicit basis using the Air Pollution Emission Experiments and Policy (APEEP) model, version AP3, and mortality risk is monetized using a \$8.7 million value of reduced mortality risk [46].

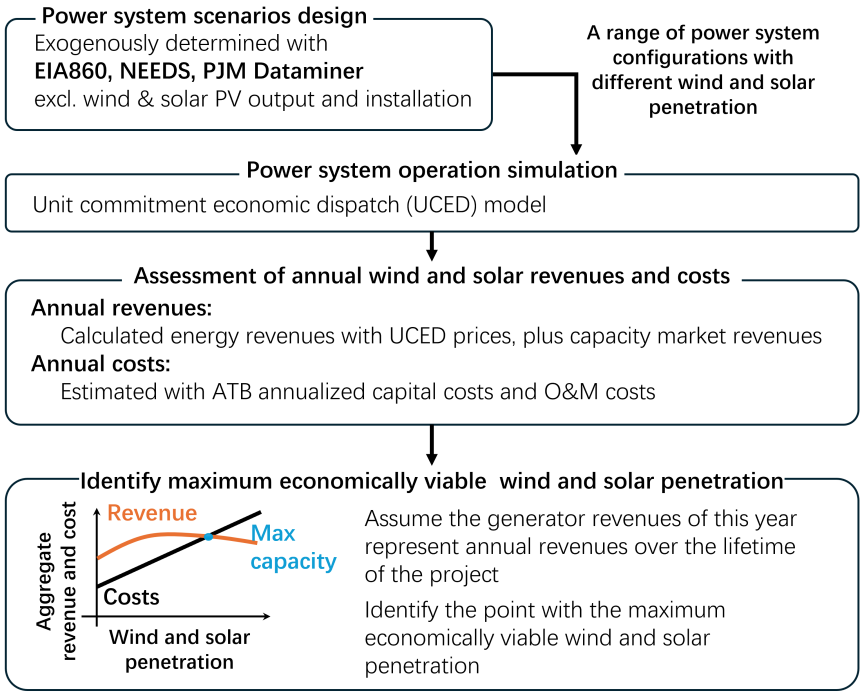


Figure 4: An explanatory diagram of how we translate short-term operational results into long-term capacity investment decisions.

4.5. Assessment of induced wind and solar capacity investment

Short-term operational results are translated to long-term structural changes in the power system (see Figure 4). Annual operational results are produced for a range of wind and solar penetrations. The penetration level where the annual revenues of wind and solar generators are equal to their annual costs is then identified. The penetration level of revenue-cost equilibrium is used to represent the maximum penetration level.

Solar and wind generators have negligible variable costs, and therefore marginal generating costs, in the short term. However, fixed costs, which equal annualized capital expenditures plus fixed operation and maintenance (O&M) costs, need to be covered by revenues for wind and solar generators to maintain profitable. To assess the profitability of wind and solar generators, we define net profits as the sum of revenues minus annual fixed costs. We assume wind and solar generators have two revenue streams: income from the energy market and income from PJM's capacity market. We assume the 1 year's operation repeats throughout generators' lifetime, as most capacity expansion models do. Hence the revenue-cost balance represents its full lifecycle economic viability.

To estimate energy market revenues, we obtain hourly electricity prices for each of our five regions from our UCED model. These regional prices are the Lagrange multipliers of each region's energy balance constraint, which represent the marginal cost of supplying additional load in each region. By summing the product of hourly regional electricity prices and regional generation for wind and for solar, we determine total annual revenues by type in each region from the energy

market. To estimate capacity market revenues, we use market mechanisms from PJM's capacity market, or its Reliability Pricing Model (RPM) [67]. Though the capacity value of wind and solar generators may decrease as penetration increases, it remains uncertain how the capacity market assesses the contribution of wind and solar sources [8, 68]. PJM derates capacity offers from generators based on their effective load carrying capability (ELCC), which reflects generator variability and availability throughout the year. PJM sets the ELCC at 0.15, 0.40, 0.38 for onshore wind, offshore wind and solar PV, respectively [69]. Wind ELCC is set at 0.233 as onshore wind accounts for one third of wind capacity expansion. We estimate wind and solar revenues from the capacity market as the product of capacity, the prior ELCC values (assuming the same value for onshore and offshore wind), and the latest average capacity market clearing price (USD 28.92/MW per day) [69]. Regional wind and solar revenues and costs are summed to obtain PJM-wide revenues and costs, which we present in our results.

For computational tractability, we assume system prices, and therefore generator revenues, over this year represent annual prices and revenues over the lifetime of the project, a similarly myopic assumption as in capacity expansion models that sample periods from a single year for making investment decisions.

We obtain fixed wind and solar costs from the National Renewable Energy Laboratory's Annual Technology Baseline (ATB) for year 2030 [70]. As we model year 2035, fixed costs at 2030 would be reasonably representative of fleet average, being the midpoint between the present and the scenario year. Annualized fixed costs are calculated with a real discount rate of 5% and a cost recovery period of 30 years [70].

To capture uncertainty in future wind and solar costs, we test the sensitivity of our results to conservative, best-guess, and optimistic ATB cost scenarios, which we refer to as high, mid, and low cost, respectively.[70].

Between the 25 wind and solar capacity levels run for each PEV scenario, we interpolate wind and solar revenues. We find the intersection of fixed costs and revenues and round down the total capacity of wind and solar to the nearest point. And at that point the combined wind and solar capacity installation reaches its maximum profitable level.

4.6. Sensitivity analysis

We run sensitivity analyses to test model sensitivity to our assumptions: 1) exogenous stationary storage capacity; 2) exogenous transmission capacity; 3) fixed wind-to-solar capacity ratio; 4) the size of PEV fleet being 10% of the light-duty vehicle fleet.

To keep the computational burden of this study tractable, stationary storage capacity and transmission capacity are assumed to be fixed. However, in the real world, the power system will see expansion in stationary storage capacity and transmission capacity that accompanies the expansion of wind and solar. Hence, we run sensitivity analyses with high transmission capacity and with high stationary storage capacity. In the high transmission scenario, the transmission capacity between each region of PJM is doubled. In the high stationary storage scenario, the capacity of battery storage is expanded from 5.4 GW (46 GWh), to 14 GW (56 GWh), by doubling the capacity of the largest battery storage unit in each region. For regions with pumped hydro

storage and without planned battery storage, a 4-hr battery storage unit with the power capacity of the largest pumped hydro storage unit is installed.

Meanwhile, we tested model sensitivity on the fixed wind-to-solar capacity ratio assumption. We assume wind and solar capacity will expand at a fixed ratio, whereas in the real world, the capacity expansion may be more strategic. We run scenarios with different wind-to-solar capacity ratios: a high wind scenario with a wind-to-solar capacity ratio of 1.46 and a high solar scenario with 0.93.

We also tested model sensitivity on the size of the PEV fleet. As PEV penetration rises, the benefits of PEV charging and charging interventions have diminishing returns. We run a high PEV penetration scenario where PEV penetration is doubled from 10% in the base case to 20%.

Acknowledgements

This work was supported in part by the Department of Engineering and Public Policy and the Department of Mechanical Engineering at Carnegie Mellon University. Craig thanks the School for Environment and Sustainability at the University of Michigan for funding.

Declaration of Interests

The authors declare no competing interests.

Author Contributions

J.C., M.C., J.M., M.B., and P.V. contributed to designing the research. J.C., M.C., J.M., and P.V. contributed to analyzing results and writing the paper. J.C. performed the research with input from coauthors.

References

[1] O. Alsauskas, E. Connelly, A. Daou, A. Gouy, M. Huismans, J.-B. Le Marois, S. McDonagh, A. Petropoulos, J. Teter, E. Jenness, J. J. Copier, T. Lombardo, V. O'Riordan, J. Sery, Global EV Outlook 2024 Moving towards increased affordability, Tech. rep. (Apr. 2024).
URL https://iea.blob.core.windows.net/assets/a9e3544b-0b12-4e15-b407-65f5c8ce1b5f/GlobalEVOutlook2024.pdf

[2] J. Archsmith, E. Muehlegger, D. S. Rapson, Future Paths of Electric Vehicle Adoption in the United States: Predictable Determinants, Obstacles, and Opportunities, Environmental and Energy Policy and the Economy 3 (2022) 71–110, publisher: The University of Chicago Press. doi:10.1086/717219.
URL https://www.journals.uchicago.edu/doi/full/10.1086/717219

[3] P. Gagnon, M. Brown, D. Steinberg, P. Brown, S. Awara, V. Carag, S. Cohen, W. Cole, J. Ho, S. Inskeep, 2022 Standard Scenarios Report: A US Electricity Sector Outlook, Tech. rep., National Renewable Energy Lab.(NREL), Golden, CO (United States) (2022).

[4] Mitigation Pathways Compatible with 1.5°C in the Context of Sustainable Development, in: Intergovernmental Panel on Climate Change (IPCC) (Ed.), Global Warming of 1.5°C: IPCC Special Report on Impacts of Global Warming of 1.5°C above Pre-industrial Levels in Context of Strengthening Response to Climate Change, Sustainable Development, and Efforts to Eradicate Poverty, Cambridge University Press, Cambridge, 2022, pp. 93–174. doi:10.1017/9781009157940.004.
URL https://www.cambridge.org/core/books/global-warming-of-15c/mitigation-pathways-compatible-with-15c-in-the-context-of-sustainable-development/051AC891C0952E62DEF2510593BC1C10

[5] R. H. Wiser, A. Mills, J. Seel, T. Levin, A. Botterud, Impacts of Variable Renewable Energy on Bulk Power System Assets, Pricing, and Costs, Tech. rep., Lawrence Berkeley National Lab. (LBNL), Berkeley, CA (United States) (Nov. 2017). doi:10.2172/1411668.
URL https://www.osti.gov/biblio/1411668

[6] X. Chen, H. Zhang, Z. Xu, C. P. Nielsen, M. B. McElroy, J. Lv, Impacts of fleet types and charging modes for electric vehicles on emissions under different penetrations of wind power, Nature Energy 3 (5) (2018) 413–421, publisher: Nature Publishing Group.

[7] A. Weis, P. Jaramillo, J. Michalek, Consequential life cycle air emissions externalities for plug-in electric vehicles in the PJM interconnection, Environmental Research Letters 11 (2) (2016) 024009, publisher: IOP Publishing. doi:10.1088/1748-9326/11/2/024009.
URL https://dx.doi.org/10.1088/1748-9326/11/2/024009

[8] A. D. Mills, T. Levin, R. Wiser, J. Seel, A. Botterud, Impacts of variable renewable energy on wholesale markets and generating assets in the United States: A review of expectations and evidence, Renewable and Sustainable Energy Reviews 120 (2020) 109670. doi:10.1016/j.rser.2019.109670.
URL https://www.sciencedirect.com/science/article/pii/S1364032119308755

[9] S. Das, E. Hittinger, E. Williams, Learning is not enough: Diminishing marginal revenues and increasing abatement costs of wind and solar, Renewable Energy 156 (2020) 634–644. doi:10.1016/j.renene.2020.03.082.
URL https://www.sciencedirect.com/science/article/pii/S0960148120304079

[10] M. T. Craig, P. Jaramillo, B.-M. Hodge, N. J. Williams, E. Severnini, A retrospective analysis of the market price response to distributed photovoltaic generation in California, Energy Policy 121 (2018) 394–403. doi:10.1016/j.enpol.2018.05.061.
URL https://www.sciencedirect.com/science/article/pii/S0301421518303781

[11] L. Bird, J. Cochran, X. Wang, Wind and Solar Energy Curtailment: Experience and Practices in the United States, Tech. rep., National Renewable Energy Lab. (NREL), Golden, CO (United States) (2014).

[12] L. E. Jones, Renewable energy integration: practical management of variability, uncertainty, and flexibility in power grids, Academic press, 2017.
URL https://www.google.com/books?hl=zh-CN&lr=&id=b_6pDQAAQBAJ&oi=fnd&

pg=PP1&dq=Flexibility+in+21st+Century+Power+Systems&ots=uFNkIQB0EG&sig=P1KbKXppuWZM4KnJyX-sjKy07QM

[13] B. Kroposki, B. Johnson, Y. Zhang, V. Gevorgian, P. Denholm, B.-M. Hodge, B. Hannegan, Achieving a 100% Renewable Grid: Operating Electric Power Systems with Extremely High Levels of Variable Renewable Energy, IEEE Power and Energy Magazine 15 (2) (2017) 61–73, conference Name: IEEE Power and Energy Magazine. doi:10.1109/MPE.2016.2637122.
URL https://ieeexplore.ieee.org/document/7866938

[14] S. Impram, S. V. Nese, B. Oral, Challenges of renewable energy penetration on power system flexibility: A survey, Energy Strategy Reviews 31 (2020) 100539, publisher: Elsevier.
URL https://www.sciencedirect.com/science/article/pii/S2211467X20300924

[15] T. Mai, P. Denholm, P. Brown, W. Cole, E. Hale, P. Lamers, C. Murphy, M. Ruth, B. Sergi, D. Steinberg, S. F. Baldwin, Getting to 100%: Six strategies for the challenging last 10%, Joule 6 (9) (2022) 1981–1994. doi:10.1016/j.joule.2022.08.004.
URL https://www.sciencedirect.com/science/article/pii/S2542435122004056

[16] B. Tarroja, L. Zhang, V. Wifvat, B. Shaffer, S. Samuelsen, Assessing the stationary energy storage equivalency of vehicle-to-grid charging battery electric vehicles, Energy 106 (2016) 673–690. doi:10.1016/j.energy.2016.03.094.
URL https://www.sciencedirect.com/science/article/pii/S0360544216303383

[17] P. Nunes, M. C. Brito, Displacing natural gas with electric vehicles for grid stabilization, Energy 141 (2017) 87–96. doi:10.1016/j.energy.2017.09.064.
URL https://www.sciencedirect.com/science/article/pii/S0360544217315852

[18] K. E. Forrest, B. Tarroja, L. Zhang, B. Shaffer, S. Samuelsen, Charging a renewable future: The impact of electric vehicle charging intelligence on energy storage requirements to meet renewable portfolio standards, Journal of Power Sources 336 (2016) 63–74. doi:10.1016/j.jpowsour.2016.10.048.
URL https://www.sciencedirect.com/science/article/pii/S0378775316314409

[19] A. Weis, J. J. Michalek, P. Jaramillo, R. Lueken, Emissions and Cost Implications of Controlled Electric Vehicle Charging in the U.S. PJM Interconnection, Environmental Science & Technology 49 (9) (2015) 5813–5819. doi:10.1021/es505822f.
URL https://pubs.acs.org/doi/10.1021/es505822f

[20] M. Bruchon, Z. L. Chen, J. Michalek, Cleaning up while Changing Gears: The Role of Battery Design, Fossil Fuel Power Plants, and Vehicle Policy for Reducing Emissions in the Transition to Electric Vehicles, Environmental Science & TechnologyPublisher: American Chemical Society (Feb. 2024). doi:10.1021/acs.est.3c07098.
URL https://doi.org/10.1021/acs.est.3c07098

[21] S. P. Holland, E. T. Mansur, N. Z. Muller, A. J. Yates, Are There Environmental Benefits from Driving Electric Vehicles? The Importance of Local Factors, American Economic Review 106 (12) (2016) 3700–3729. doi:10.1257/aer.20150897.
URL https://www.aeaweb.org/articles?id=10.1257/aer.20150897

[22] S. P. Holland, E. T. Mansur, N. Z. Muller, A. J. Yates, Distributional Effects of Air Pollution from Electric Vehicle Adoption, Journal of the Association of Environmental and Resource Economists 6 (S1) (2019) S65–S94, publisher: The University of Chicago Press. doi:10.1086/701188.
URL https://www.journals.uchicago.edu/doi/abs/10.1086/701188

[23] S. P. Holland, E. T. Mansur, N. Z. Muller, A. J. Yates, Decompositions and Policy Consequences of an Extraordinary Decline in Air Pollution from Electricity Generation, American Economic Journal: Economic Policy 12 (4) (2020) 244–274. doi:10.1257/pol.20190390.
URL https://www.aeaweb.org/articles?id=10.1257/pol.20190390

[24] S. P. Holland, M. J. Kotchen, E. T. Mansur, A. J. Yates, Why marginal CO2 emissions are not decreasing for US electricity: Estimates and implications for climate policy, Proceedings of the National Academy of Sciences 119 (8) (2022) e2116632119, publisher: Proceedings of the National Academy of Sciences. doi:10.1073/pnas.2116632119.
URL https://www.pnas.org/doi/abs/10.1073/pnas.2116632119

[25] R. Tu, Y. J. Gai, B. Farooq, D. Posen, M. Hatzopoulou, Electric vehicle charging optimization to minimize marginal greenhouse gas emissions from power generation, Applied Energy 277 (2020) 115517. doi:10.1016/j.apenergy.2020.115517.
URL http://www.sciencedirect.com/science/article/pii/S0306261920310291

[26] M. Wang, M. T. Craig, The value of vehicle-to-grid in a decarbonizing California grid, Journal of Power Sources 513 (2021) 230472. doi:10.1016/j.jpowsour.2021.230472.
URL https://www.sciencedirect.com/science/article/pii/S0378775321009757

[27] R. Shi, S. Li, P. Zhang, K. Y. Lee, Integration of renewable energy sources and electric vehicles in V2G network with adjustable robust optimization, Renewable Energy 153 (2020) 1067–1080. doi:10.1016/j.renene.2020.02.027.
URL https://www.sciencedirect.com/science/article/pii/S0960148120302135

[28] N. A. Ryan, J. X. Johnson, G. A. Keoleian, Comparative Assessment of Models and Methods To Calculate Grid Electricity Emissions, Environmental Science & Technology 50 (17) (2016) 8937–8953, publisher: American Chemical Society. doi:10.1021/acs.est.5b05216.
URL https://doi.org/10.1021/acs.est.5b05216

[29] P. J. Gagnon, J. E. T. Bistline, M. H. Alexander, W. J. Cole, Short-run marginal emission rates omit important impacts of electric-sector interventions, Proceedings of the National Academy of Sciences 119 (49) (2022) e2211624119, publisher: Proceedings of the National Academy of Sciences. doi:10.1073/pnas.2211624119.
URL https://www.pnas.org/doi/full/10.1073/pnas.2211624119

[30] S. P. Holland, E. T. Mansur, A. Yates, Decarbonization and Electrification in the Long Run (May 2022).
URL https://papers.ssrn.com/abstract=4122811

[31] T. Brown, D. Schlachtberger, A. Kies, S. Schramm, M. Greiner, Synergies of sector coupling and transmission reinforcement in a cost-optimised, highly renewable European energy sys-

tem, Energy 160 (2018) 720–739. doi:10.1016/j.energy.2018.06.222.
URL https://www.sciencedirect.com/science/article/pii/S036054421831288X

[32] J. Owens, I. Miller, E. Gençer, Can vehicle-to-grid facilitate the transition to low carbon energy systems?, Energy Advances 1 (12) (2022) 984–998, publisher: Royal Society of Chemistry. doi:10.1039/D2YA00204C.
URL https://pubs.rsc.org/en/content/articlelanding/2022/ya/d2ya00204c

[33] F. Manríquez, E. Sauma, J. Aguado, S. de la Torre, J. Contreras, The impact of electric vehicle charging schemes in power system expansion planning, Applied Energy 262 (2020) 114527. doi:10.1016/j.apenergy.2020.114527.
URL https://www.sciencedirect.com/science/article/pii/S0306261920300398

[34] A. Weis, P. Jaramillo, J. Michalek, Estimating the potential of controlled plug-in hybrid electric vehicle charging to reduce operational and capacity expansion costs for electric power systems with high wind penetration, Applied Energy 115 (2014) 190–204. doi:10.1016/j.apenergy.2013.10.017.
URL https://www.sciencedirect.com/science/article/pii/S0306261913008374

[35] U. Nopmongcol, J. Grant, E. Knipping, M. Alexander, R. Schurhoff, D. Young, J. Jung, T. Shah, G. Yarwood, Air Quality Impacts of Electrifying Vehicles and Equipment Across the United States, Environmental Science & Technology 51 (5) (2017) 2830–2837, publisher: American Chemical Society. doi:10.1021/acs.est.6b04868.
URL https://doi.org/10.1021/acs.est.6b04868

[36] C. J. R. Sheppard, A. T. Jenn, J. B. Greenblatt, G. S. Bauer, B. F. Gerke, Private versus Shared, Automated Electric Vehicles for U.S. Personal Mobility: Energy Use, Greenhouse Gas Emissions, Grid Integration, and Cost Impacts, Environmental Science & Technology 55 (5) (2021) 3229–3239, publisher: American Chemical Society. doi:10.1021/acs.est.0c06655.
URL https://doi.org/10.1021/acs.est.0c06655

[37] P. Gagnon, W. Cole, Planning for the evolution of the electric grid with a long-run marginal emission rate, iScience 25 (3) (2022) 103915. doi:10.1016/j.isci.2022.103915.
URL https://www.sciencedirect.com/science/article/pii/S2589004222001857

[38] A. Jenn, Emissions of electric vehicles in California's transition to carbon neutrality, Applied Energy 339 (2023) 120974. doi:10.1016/j.apenergy.2023.120974.
URL https://www.sciencedirect.com/science/article/pii/S0306261923003380

[39] S. P. Holland, E. T. Mansur, V. Verdier, A. J. Yates, Regularization from Economic Constraints: A New Estimator for Marginal Emissions (Jan. 2024). doi:10.3386/w32065.
URL https://www.nber.org/papers/w32065

[40] R. Lueken, J. Apt, The effects of bulk electricity storage on the PJM market, Energy Systems 5 (4) (2014) 677–704. doi:10.1007/s12667-014-0123-7.
URL https://doi.org/10.1007/s12667-014-0123-7

[41] J. Chen, F. Wang, X. He, X. Liang, J. Huang, S. Zhang, Y. Wu, Emission mitigation potential from coordinated charging schemes for future private electric vehicles, Applied Energy 308 (2022) 118385. doi:10.1016/j.apenergy.2021.118385.
URL https://www.sciencedirect.com/science/article/pii/S0306261921016238

[42] M. Carrión, R. Domínguez, R. Zárate-Miñano, Influence of the controllability of electric vehicles on generation and storage capacity expansion decisions, Energy 189 (2019) 116156. doi:10.1016/j.energy.2019.116156.
URL https://www.sciencedirect.com/science/article/pii/S0360544219318511

[43] C. J. R. Sheppard, G. S. Bauer, B. F. Gerke, J. B. Greenblatt, A. T. Jenn, A. R. Gopal, Joint Optimization Scheme for the Planning and Operations of Shared Autonomous Electric Vehicle Fleets Serving Mobility on Demand, Transportation Research Record 2673 (6) (2019) 579–597, publisher: SAGE Publications Inc. doi:10.1177/0361198119838270.
URL https://doi.org/10.1177/0361198119838270

[44] PJM - Serial Service Request Status (2024).
URL https://www.pjm.com/planning/service-requests/serial-service-request-status

[45] EPA Report on the Social Cost of Greenhouse Gases: Estimates Incorporating Recent Scientific Advances, Tech. rep. (Nov. 2023).

[46] K. Clay, A. Jha, N. Muller, R. Walsh, External Costs of Transporting Petroleum Products: Evidence from Shipments of Crude Oil from North Dakota by Pipelines and Rail, The Energy Journal 40 (1) (2019) 55–72. doi:10.5547/01956574.40.1.kcla.
URL https://journals.sagepub.com/doi/10.5547/01956574.40.1.kcla

[47] PJM, Energy Transition in PJM: Frameworks for Analysis, Tech. rep. (Dec. 2021).
URL https://pjm.com/-/media/committees-groups/committees/mrc/2021/20211215/20211215-item-09-energy-transition-in-pjm-whitepaper.ashx

[48] P. Gasper, A. Saxon, Y. Shi, E. Endler, K. Smith, F. M. Thakkar, Degradation and modeling of large-format commercial lithium-ion cells as a function of chemistry, design, and aging conditions, Journal of Energy Storage 73 (2023) 109042. doi:10.1016/j.est.2023.109042.
URL https://www.sciencedirect.com/science/article/pii/S2352152X23024404

[49] N. R. Chowdhury, A. J. Smith, K. Frenander, A. Mikheenkova, R. W. Lindström, T. Thiringer, Influence of state of charge window on the degradation of Tesla lithium-ion battery cells, Journal of Energy Storage 76 (2024) 110001. doi:10.1016/j.est.2023.110001.
URL https://www.sciencedirect.com/science/article/pii/S2352152X2303400X

[50] A. Leippi, M. Fleschutz, K. Davis, A.-L. Klingler, M. D. Murphy, Optimizing electric vehicle fleet integration in industrial demand response: Maximizing vehicle-to-grid benefits while compensating vehicle owners for battery degradation, Applied Energy 374 (2024) 123995. doi:10.1016/j.apenergy.2024.123995.
URL https://www.sciencedirect.com/science/article/pii/S0306261924013783

[51] S. Sagaria, M. van der Kam, T. Boström, Vehicle-to-grid impact on battery degradation and estimation of V2G economic compensation, Applied Energy 377 (2025) 124546. doi:10.1016/j.apenergy.2024.124546.
URL https://www.sciencedirect.com/science/article/pii/S0306261924019299

[52] J. Gong, D. Wasylowski, J. Figgener, S. Bihn, F. Rücker, F. Ringbeck, D. U. Sauer, Quantifying the impact of V2X operation on electric vehicle battery degradation: An experimental evaluation, eTransportation 20 (2024) 100316. doi:10.1016/j.etran.2024.100316.
URL https://www.sciencedirect.com/science/article/pii/S2590116824000067

[53] M. Naumann, Techno-economic evaluation of stationary battery energy storage systems with special consideration of aging, Ph.D. thesis, Technische Universität München (2018).
URL https://mediatum.ub.tum.de/1434981

[54] M. Naumann, F. B. Spingler, A. Jossen, Analysis and modeling of cycle aging of a commercial LiFePO4/graphite cell, Journal of Power Sources 451 (2020) 227666. doi:10.1016/j.jpowsour.2019.227666.
URL https://www.sciencedirect.com/science/article/pii/S0378775319316593

[55] A. Silverman, Z. Wendling, K. Rizal, Outlook for Pending Generation in the PJM Interconnection Queue, Tech. rep. (May 2024).
URL https://www.energypolicy.columbia.edu/publications/outlook-for-pending-generation-in-the-pjm-interconn

[56] Current Methods for Life Cycle Analyses of Low-Carbon Transportation Fuels in the United States, National Academies Press, Washington, D.C., 2022. doi:10.17226/26402.
URL https://www.nap.edu/catalog/26402

[57] B. Dai, H. Qi, W. Dou, S. Liu, D. Zhong, H. Yang, V. Nian, Y. Hao, Life cycle energy, emissions and cost evaluation of CO2 air source heat pump system to replace traditional heating methods for residential heating in China: System configurations, Energy Conversion and Management 218 (2020) 112954. doi:10.1016/j.enconman.2020.112954.
URL https://www.sciencedirect.com/science/article/pii/S0196890420304921

[58] S. Liu, Z. Li, B. Dai, Z. Zhong, H. Li, M. Song, Z. Sun, Energetic, economic and environmental analysis of air source transcritical CO2 heat pump system for residential heating in China, Applied Thermal Engineering 148 (2019) 1425–1439. doi:10.1016/j.applthermaleng.2018.08.061.
URL https://www.sciencedirect.com/science/article/pii/S1359431117381954

[59] P. Carroll, M. Chesser, P. Lyons, Air Source Heat Pumps field studies: A systematic literature review, Renewable and Sustainable Energy Reviews 134 (2020) 110275. doi:10.1016/j.rser.2020.110275.
URL https://www.sciencedirect.com/science/article/pii/S1364032120305621

[60] M. Muratori, Impact of uncoordinated plug-in electric vehicle charging on residential power demand, Nature Energy 3 (3) (2018) 193–201. doi:10.1038/s41560-017-0074-z.
URL http://www.nature.com/articles/s41560-017-0074-z

[61] PJM State of the Market - 2024, Tech. rep., Monitoring Analytics (2024).
URL https://www.monitoringanalytics.com/reports/PJM_State_of_the_Market/2024.shtml

[62] Form EIA-923 detailed data with previous form data (EIA-906/920) - U.S. Energy Information Administration (EIA) (2024).
URL https://www.eia.gov/electricity/data/eia923/

[63] O. US EPA, National Electric Energy Data System (NEEDS) (Apr. 2018).
URL https://www.epa.gov/power-sector-modeling/national-electric-energy-data-system-needs

[64] Data Miner 2 (2024).
URL https://dataminer2.pjm.com/

[65] Form EIA-860 detailed data with previous form data (EIA-860A/860B) (2024).
URL https://www.eia.gov/electricity/data/eia860/

[66] O. US EPA, National Emissions Inventory (NEI) (Jun. 2015).
URL https://www.epa.gov/air-emissions-inventories/national-emissions-inventory-nei

[67] PJM, PJM Manual 18: PJM Capacity Market, Tech. rep. (Feb. 2023).

[68] P. C. Bhagwat, K. K. Iychettira, J. C. Richstein, E. J. L. Chappin, L. J. De Vries, The effectiveness of capacity markets in the presence of a high portfolio share of renewable energy sources, Utilities Policy 48 (2017) 76–91. doi:10.1016/j.jup.2017.09.003.
URL https://www.sciencedirect.com/science/article/pii/S0957178716300406

[69] 2023/2024 BRA Effective Load Carrying Capability (ELCC) Class Ratings, Tech. rep. (2021).
URL https://www.pjm.com/-/media/planning/res-adeq/elcc/elcc-class-ratings-for-2023-2024-bra.ashx

[70] L. Vimmerstedt, T. Stehly, S. Akar, A. Sekar, B. Mirletz, D. Stright, C. Augustine, P. Beiter, P. Bhaskar, N. Blair, S. Cohen, W. Cole, P. Duffy, D. Feldman, P. Gagnon, P. Kurup, C. Murphy, V. Ramasamy, J. Robins, J. Zuboy, D. Oladosu, J. Hoffmann, 2022 Annual Technology Baseline (ATB) Cost and Performance Data for Electricity Generation Technologies, Tech. Rep. 5716, DOE Open Energy Data Initiative (OEDI); National Renewable Energy Laboratory (NREL) (Jun. 2022). doi:10.25984/1871952.
URL https://www.osti.gov/dataexplorer/biblio/dataset/1871952

Contents

1 Introduction **2**

Introduction **2**

2 Results **3**

2.1 Wind and solar capacity investment induced by PEV charging 3

Wind and solar capacity investment induced by PEV charging **3**

2.2 Electricity generation induced by PEV charging 4

Electricity generation induced by PEV charging **4**

2.3 Air emission externalities induced by PEV charging 6

Air emission externality costs **6**

2.4 Sensitivity analysis 9

3 Discussion and Limitations **11**

Discussion and Limitations **11**

3.1 Limitations and caveats 11

3.2 Discussion 12

4 Materials and Methods **13**

Materials and Methods **13**

4.1 PEV behavioral model 13

4.2 Power system model 14

4.3 Power system scenarios and data sources 15

4.4 Air emission externality costs 16

4.5 Assessment of induced wind and solar capacity investment 17

4.6 Sensitivity analysis 18

References **19**

Supplementary Information for 'Negative Electric Vehicle Emissions: Vehicle-to-Grid Incentivizes Enough Wind and Solar Investment to Reverse EV Charging Emissions'

Jiahui Chen[a,b], Michael T. Craig[a,c], Jeremy Michalek **[b,d,e], Matthew Bruchon[b], Parth Vaishnav[a]

[a]*School for Environment and Sustainability, University of Michigan, Ann Arbor, MI 48109, USA*

[b]*Department of Engineering and Public Policy, Carnegie Mellon University, Pittsburgh, PA 15213, USA*

[c]*Department of Industrial and Operations Engineering, University of Michigan, Ann Arbor, MI 48109, USA*

[d]*Department of Mechanical Engineering, Carnegie Mellon University, Pittsburgh, PA 15213, USA*

[e]*Department of Civil and Environmental Engineering, Carnegie Mellon University, Pittsburgh, PA 15213, USA*

Email address: jmichalek@cmu.edu (Jeremy Michalek **)

1. Data and Code Availability

Data and code used in this research are stored on a public repository (https://github.com/jia-hui-chen0/Long-term-emission-effects-of-grid-intervention.git)

2. Supplementary Literature Review

This section provides supplementary literature review to the main body (1). Current studies assess emission impacts of plug-in electric vehicle adoption and charging interventions mainly with two approaches, focusing either on the power system operation or on the power system capacity expansion. The first approach assesses emission impacts induced by grid intervention with a fixed power system[1–6]. Tu et al. 2020 and Holland et al. 2022 used marginal emission factors to evaluate emission impacts of PEV charging intervention.[1, 2] Chen et al. 2018 used a power system dispatch model to assess the emission impacts of charging intervention in fixed power systems [7]. However, Owens et al. and Gagnon et al. [8, 9] note that, in the long run, grid interventions like EV adoption can induce changes in the trajectory of power system generator capacity expansion, and this structural change of the power system also has climate implications.

Other relevant studies employ capacity expansion models (CEMs). However, CEMs typically do not model granular short-term power system constraints, and many of these studies make simplification assumptions about grid operation [8, 10, 11]. Brown et al. 2018 assessed cost reduction effects of grid flexibility options provided by the building sector and the transportation sector [10]. Though their model included PEV with smart charging and V2G, it represented PEV flexibility with stationary storage of 50% capacity of PEVs. This simplification can be necessary for CEMs but lacks representation of operational constraints that are vital to understanding PEV flexibility. Weis et al. 2014 managed to join the force of an operational cost model and a capacity expansion model[12]. The study ran power system simulation for 4 representative weeks of a year and used the results as inputs for a capacity expansion model. As a result, the study's scalability was limited. Moreover, the study did not model V2G. Owens et al. 2022, based on a CEM, represented V2G operation in the model with detailed operational constraints, informed by real-world travel records [8]. However, they only allow V2G to participate in the ancillary service market but not in the energy market, which limits the potential of V2G. Moreover, the study only considers a hypothetical optimal power system that is built from scratch and does not consider effects of installed fossil fuel generators on grid interventions, which, can increase system emissions with large scale deployment of energy storage and[13] While the investigation done by existing studies have been insightful and fruitful, a holistic view that combines power system operation and capacity expansion helps answer the question better, as it is the short-term operational constraints that ultimately determines the system operation outcome.

Furthermore, by ignoring transmission constraints between grid regions, along with the possibility that generation and EV loads are added in different regions, the study omits probable spatial mismatch between V2G and generation. As for the spatial nuances, V2G service is best available in load centers [14, 15], whereas much of variable renewable energy generation capacity is located in distant and rural areas [16, 17]. This mismatch of the spatial distribution of demand and supply also affects the value of grid flexibility options such as flexible PEV load.

Table 1: Comparison of method and materials of existing studies and this study. VRE is short for variable renewable energy.

Author and year	Modeling of operational constraints of grid intervention	Realistic BEV charging profiles	Endogenous capacity expansion	Consideration of existing fossil fuel generators	Analysis of impacts of grid intervention on VRE deployment	Endogenous power system operation modeling	V2G modeling
Owens et al. 2022 [8]	✓		✓		✓	✓	✓
Holland et al. 2022 [1]				✓			
Gagnon & Cole 2022 [9]			✓	✓	✓	✓	
Carrión et al. 2015 [18]	✓		✓	✓	✓		
Shi et al. 2020 [5]	✓			✓		✓	✓
Manríquez et al. 2020 [11]	✓			✓		✓	✓
Jenn et al. 2020 [19]		✓	✓	✓		✓	
Weis et al. 2014 [12]	✓	✓	✓		✓	✓	
Weis et al. 2015 [20]	✓	✓		✓	✓	✓	
Nunes & Brito 2017 [21]	✓	✓				✓	✓
Forrest et al. 2016 [22]	✓	✓		✓		✓	✓
Tarroja et al. 2016 [23]	✓	✓				✓	✓
This study	✓	✓	✓	✓	✓	✓	✓

3. Sensitivity analysis

3.1. Higher stationary storage

In the base case, the PJM power system has 5.4 GW(42 GWh) grid-scale storage units. The assumed stationary storage is constant against varying wind and solar power penetration levels. To test the robustness of our results against the addition of more stationary storage capacity, we run the analysis with more battery storage capacity, where the total stationary storage capacity is increased to 14 GW (56 GWh).

Shown in Figure 1, V2G increases the maximum profitable capacity of wind and solar capacity by 4.2 GW (a 6% increase), significantly lower than under the base case: 15 GW (from 64 GW to 79 GW, a 23% increase). As the system's demand for grid flexibility is saturated by the addition of stationary storage, benefits provided by V2G significantly diminish.

As a result of lower induced wind and solar capacity investment, the wind and solar generation changes induced by V2G under the high battery scenario are also smaller than the base case (shown in Figure 2). When induced capacity investment is considered, wind and solar generation increases (15 TWh) are much lower than under the base case (45 TWh).

Due to changes of generation mix, total system costs differ under different charging scenarios. When ignoring induced wind and solar capacity investment, total system costs under V2G are 0.20% higher than without PEVs ($13 per PEV per year increase). When accounting for induced wind and solar capacity investment, total system costs under V2G are 3% lower than without PEVs ($180 per PEV per year reduction). System cost reduction per PEV per year is 80% lower than the base case.

As a result of changes discussed above, V2G's emission externality reduction benefits are also significantly diminished (see Figure 3). When considering induced wind and solar capacity investment, V2G reduces air emission externalities by $630 per PEV, compared with $2200 under the base case.

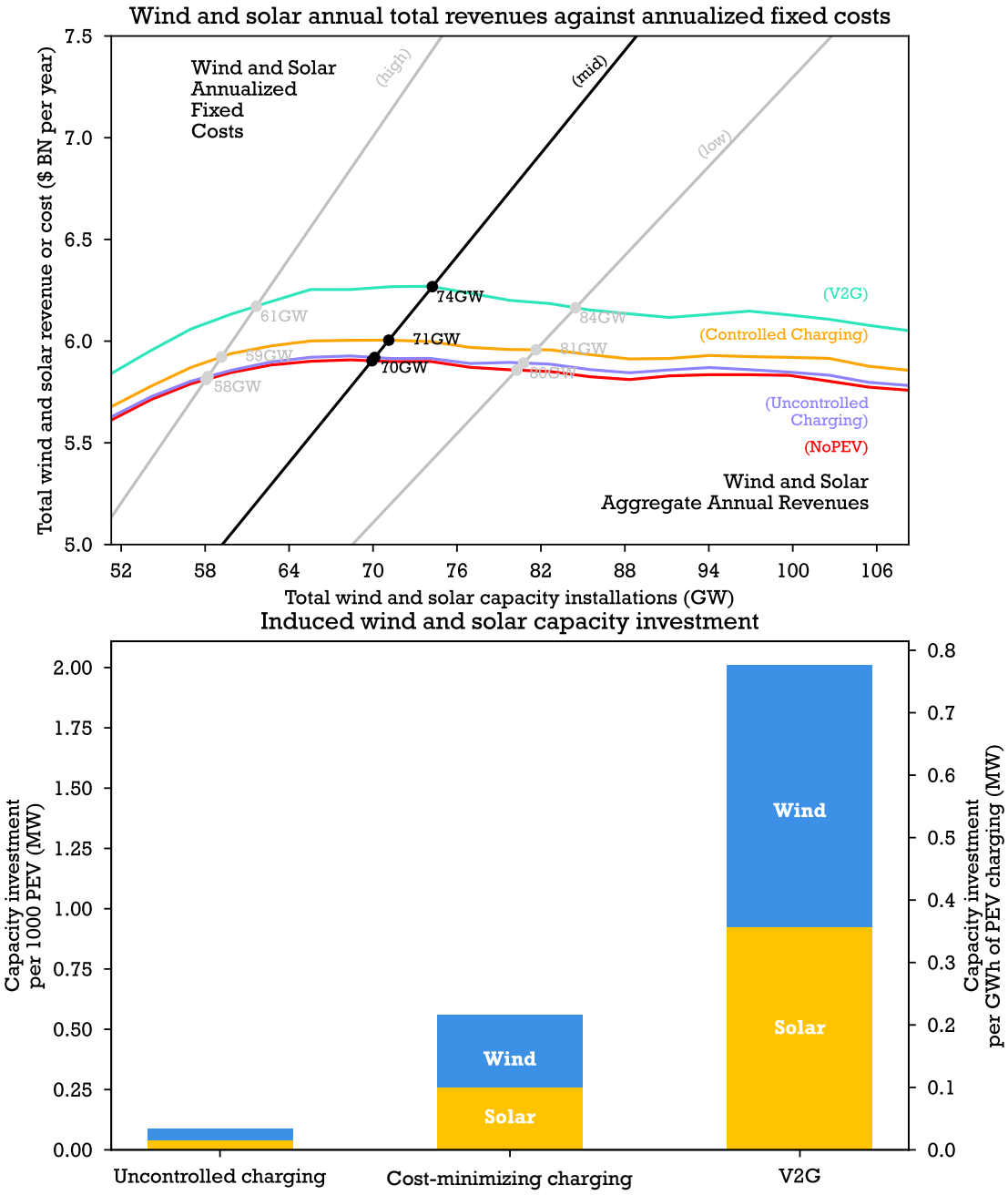


Figure 1: Effect of PEV charging load on the economics of wind and solar capacity investment. Top panel: Total revenues and total annualized fixed costs for solar and wind generators, by PEV and PEV charging intervention scenarios and by wind and solar fixed cost scenarios. **All results in this figure are run with additional stationary storage than the base case (14 GW compared with 5.4 GW).** All other parameters are the same. Note: (high): conservative fixed cost scenario, (mid): base case fixed cost scenario, (low): optimistic fixed cost scenario. Bottom panel: Wind and solar capacity investment induced by PEV charging interventions, including uncontrolled charging (UC), cost-minimizing charging (CC) and vehicle-to-grid (V2G), relative to the NoPEV baseline scenario. The currency unit is 2024 USD. $ BN is short for billion USD. Further detailed methods are described in the method section.

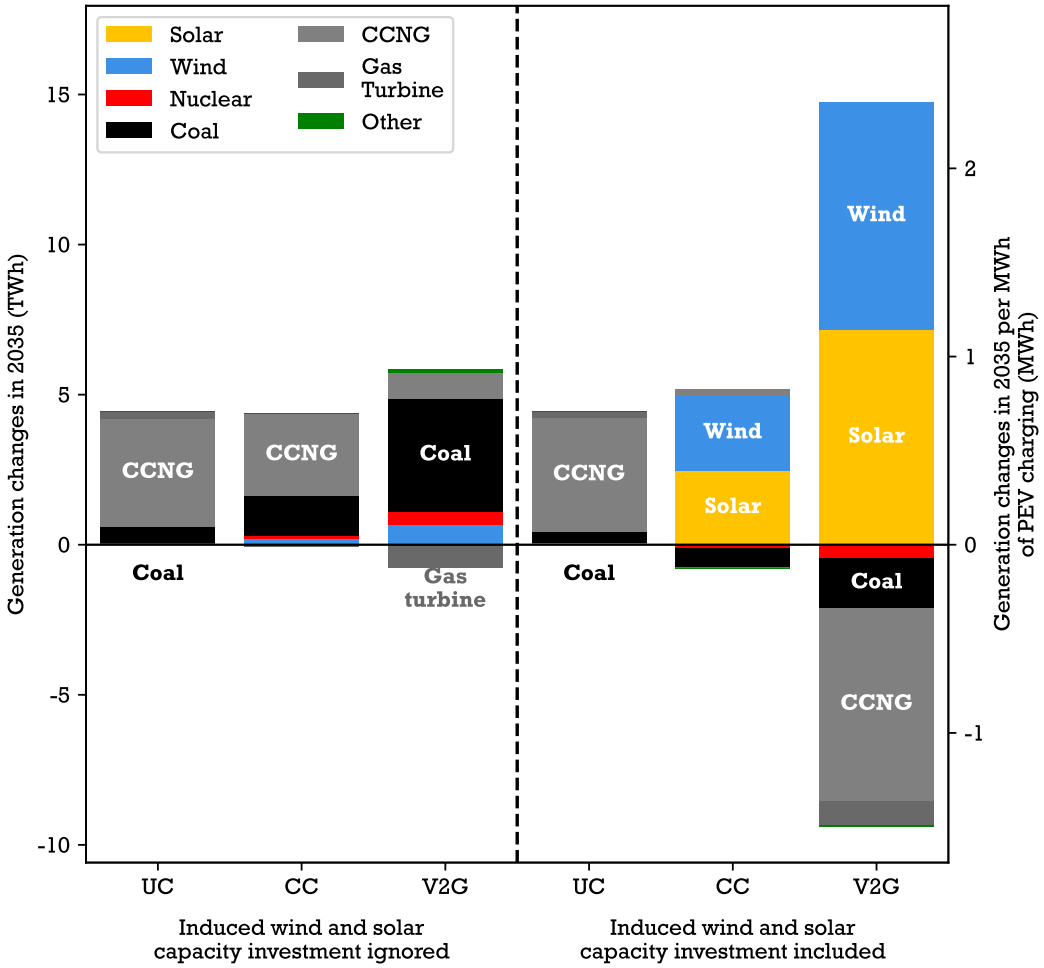


Figure 2: Effect of PEV charging load on power generation. Changes in annual generation by fuel type, relative to the NoPEV case, for each PEV charging scenario when ignoring versus including induced wind and solar capacity investment. **All results in this figure are run with additional stationary storage than the base case (14 GW compared with 5.4 GW in the base case).** All other parameters are the same. 'CCNG' fuel type includes combined cycle natural gas generators. 'Other' fuel types include biomass, fossil waste, fuel cell, hydro, landfill gas, municipal solid waste, non-fossil waste, and oil or gas steam.

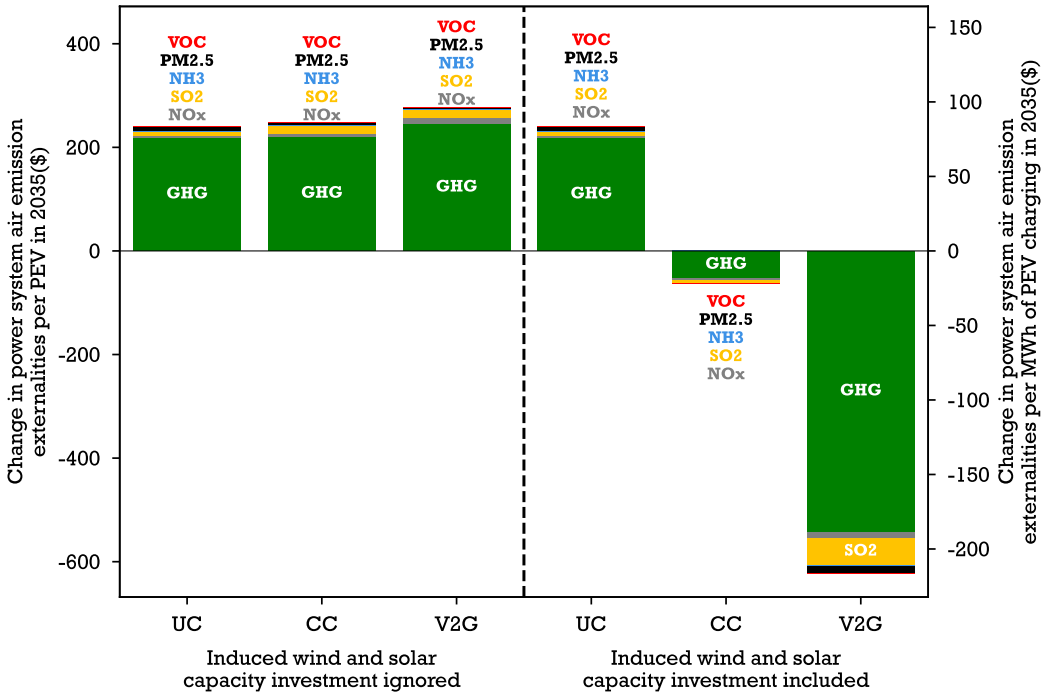


Figure 3: Effect of PEV charging on power system air emission externalities. Change in total power system air emission externalities per PEV and per MWh of PEV charging in 2035, relative to the NoPEV scenario, under each PEV charging scenario when ignoring versus including induced wind and solar capacity investment. **All results in this figure are run with additional stationary storage than the base case (14 GW compared with 5.4 GW in the base case).** The 'ignored' scenarios use generation portfolios given by PJM's grid planning study for 2035 [24]. The 'included' scenarios consider wind and solar capacity at maximum profitable capacity, as described in Method and Materials.

3.2. Higher transmission

To test the robustness of our results against the addition of more transmission capacity, we run the analysis with double the transmission capacity compared to the base case.

Shown in Figure 4, V2G increases the maximum profitable capacity of wind and solar capacity by 20 GW (from 71 GW to 91 GW, a 28% increase), higher than under the base case: 15 GW (from 64 GW to 79 GW, a 23% increase). V2G benefits from better interconnectedness with the transmission capacity expansion.

As a result of more induced wind and solar capacity investment, the wind and solar generation changes induced by V2G under the high transmission scenario are also larger than the base case (shown in Figure 5). When induced capacity investment is considered, wind and solar generation increases (55 TWh) are 22% higher than under the base case (45 TWh).

When ignoring induced wind and solar capacity investment, total system costs under V2G are 5.2% lower than without PEVs ($340 per PEV per year reduction). When accounting for induced wind and solar capacity investment, total system costs under V2G are 18% lower than without PEVs ($1100 per PEV per year reduction). System cost reduction per PEV per year is 25% higher than the base case.

As a result of changes discussed above, V2G reduces air emission externalities by $2900 per PEV, 32% higher compared with $2200 under the base case (see Figure 6).

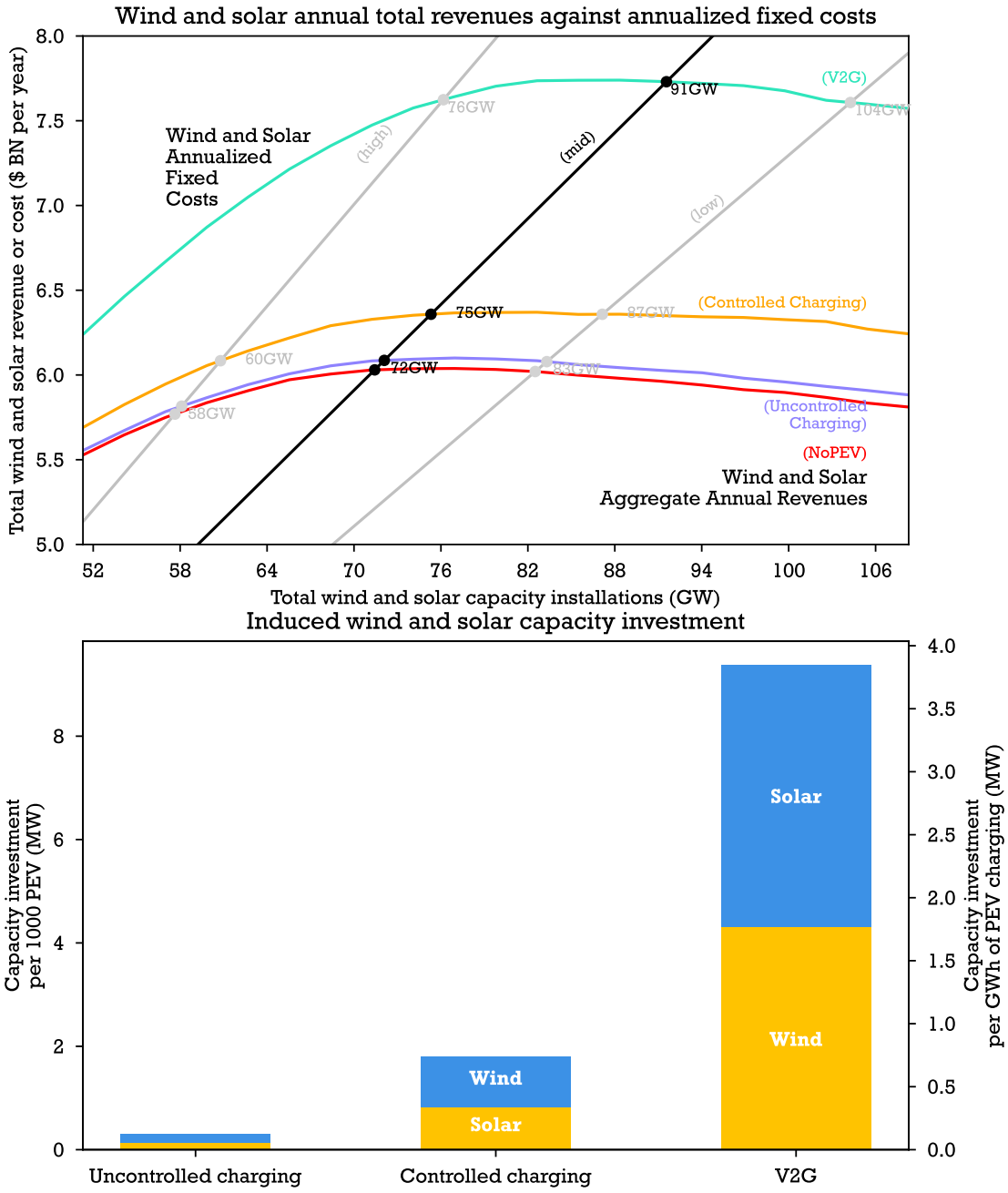


Figure 4: Effect of PEV charging load on the economics of wind and solar capacity investment. Top panel: Total revenues and total annualized fixed costs for solar and wind generators, by PEV and PEV charging intervention scenarios and by wind and solar fixed cost scenarios. **All results in this figure are run with twice as much transmission capacity as the base case.** All other parameters are the same. Note: (high): conservative fixed cost scenario, (mid): base case fixed cost scenario, (low): optimistic fixed cost scenario. Bottom panel: Wind and solar capacity investment induced by PEV charging interventions, including uncontrolled charging (UC), cost-minimizing charging (CC) and vehicle-to-grid (V2G), relative to the NoPEV baseline scenario. The currency unit is 2024 USD. $ BN is short for billion USD. Further detailed methods are described in the method section.

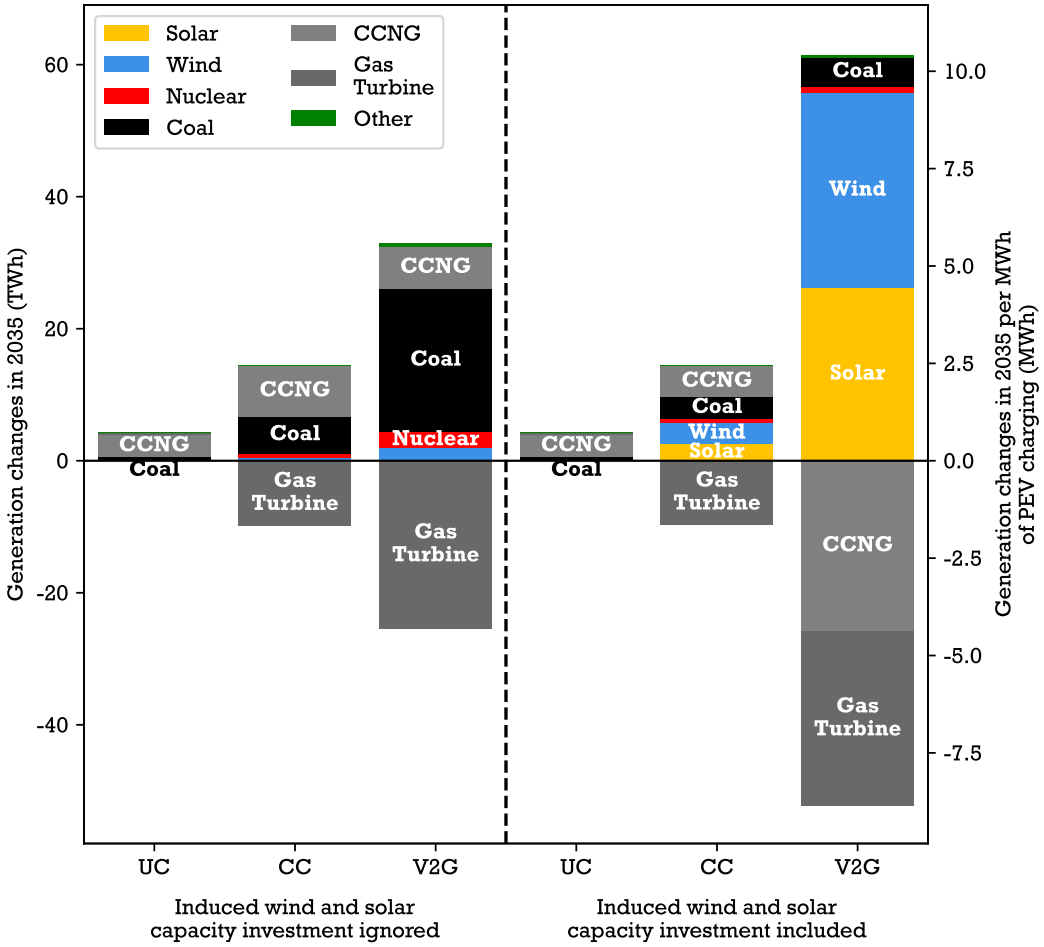


Figure 5: Effect of PEV charging load on power generation. Changes in annual generation by fuel type, relative to the NoPEV case, for each PEV charging scenario when ignoring versus including induced wind and solar capacity investment. **All results in this figure are run with twice as much transmission capacity as the base case.** All other parameters are the same. 'CCNG' fuel type includes combined cycle natural gas generators. 'Other' fuel types include biomass, fossil waste, fuel cell, hydro, landfill gas, municipal solid waste, non-fossil waste, and oil or gas steam.

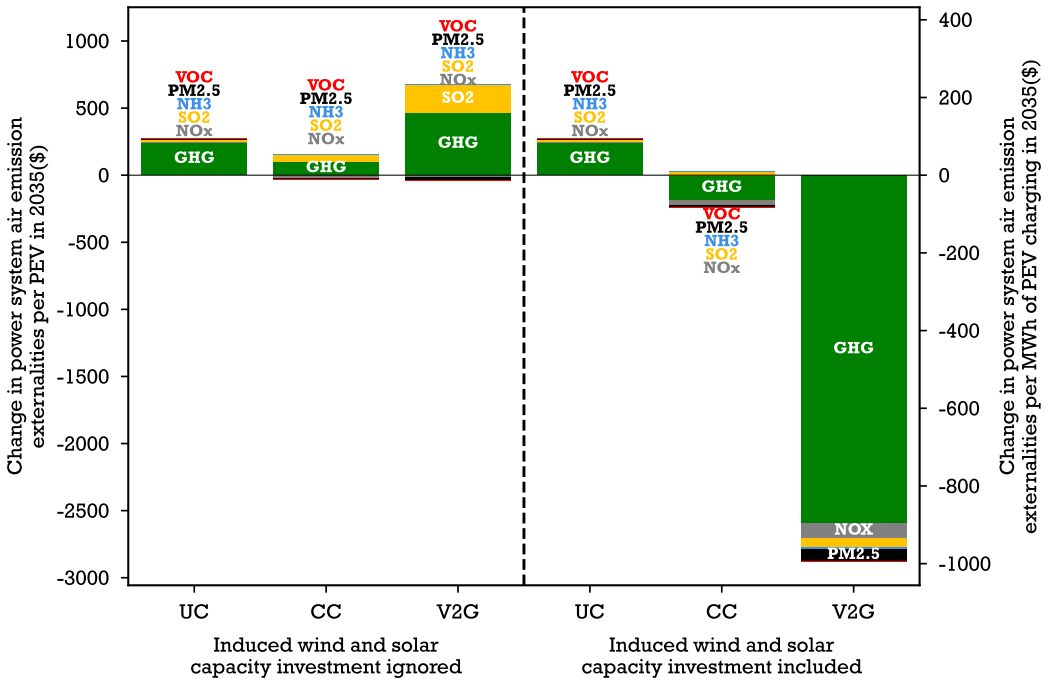


Figure 6: Effect of PEV charging on power system air emission externalities. Change in total power system air emission externalities per PEV and per MWh of PEV charging in 2035, relative to the NoPEV scenario, under each PEV charging scenario when ignoring versus including induced wind and solar capacity investment. **All results in this figure are run with twice as much transmission capacity as the base case.** The 'ignored' scenarios use generation portfolios given by PJM's grid planning study for 2035 [24]. The 'included' scenarios consider wind and solar capacity at maximum profitable capacity, as described in Method and Materials.

3.3. Higher PEV penetration

In the base case, we assume the PEV fleet accounts for 10% of PJM's light-duty passenger vehicles. To test the robustness of our results with more PEVs in the system, we run the analysis with more PEVs, where the number of PEVs is doubled.

Shown in Figure 7, with a larger PEV fleet, the total wind and solar capacity investment induced by V2G increases significantly. Under a high PEV penetration scenario, V2G increases the maximum profitable capacity of wind and solar capacity by 24 GW (a 39% increase) for a combined wind and solar capacity of 64 GW with no PEVs. The increases are 60% higher than under the base case: 15 GW (a 23% increase) increase for a combined capacity with no PEVs of 64 GW. On the per GWh charging demand basis, however, the induced capacity investments with higher PEV penetration (2.3 MW/GWh of PEV charging) are lower than the base case (2.9 MW/GWh of PEV charging). The capacity investment induction benefits of V2G are only diluted by 20% despite doubling the number of PEVs.

As a result of higher induced wind and solar capacity investment, the wind and solar generation changes induced by V2G under the high battery scenario are also higher than the base case (shown in Figure 8). When induced capacity investment is considered, wind and solar generation increases (68 TWh) are 51% higher than under the base case (45 TWh). On the per MWh of PEV charging basis, wind and solar generation increases by 5.8 MWh for every MWh of PEV charging, compared with 7.8 MWh under the base case. The wind and solar generation increase is diluted by 26% due to the addition of PEVs to the system.

When ignoring induced wind and solar capacity investment, total system costs under V2G are 5.2% lower than without PEVs ($170 per PEV per year reduction). When accounting for induced wind and solar capacity investment, total system costs under V2G are 19% lower than without PEVs ($620 per PEV per year reduction). As a result of higher wind and solar installed capacity and generation discussed above, doubling the number of PEVs also increases V2G's air emission externality reduction benefits (shown in Figure 9). With a PEV penetration of 20%, total air emission externalities are reduced by $1500 per PEV per year, 32% less compared with the base case. Though doubling the number of PEVs dilutes emission externality reduction on the per PEV basis, the benefit dilution lags behind the penetration increase.

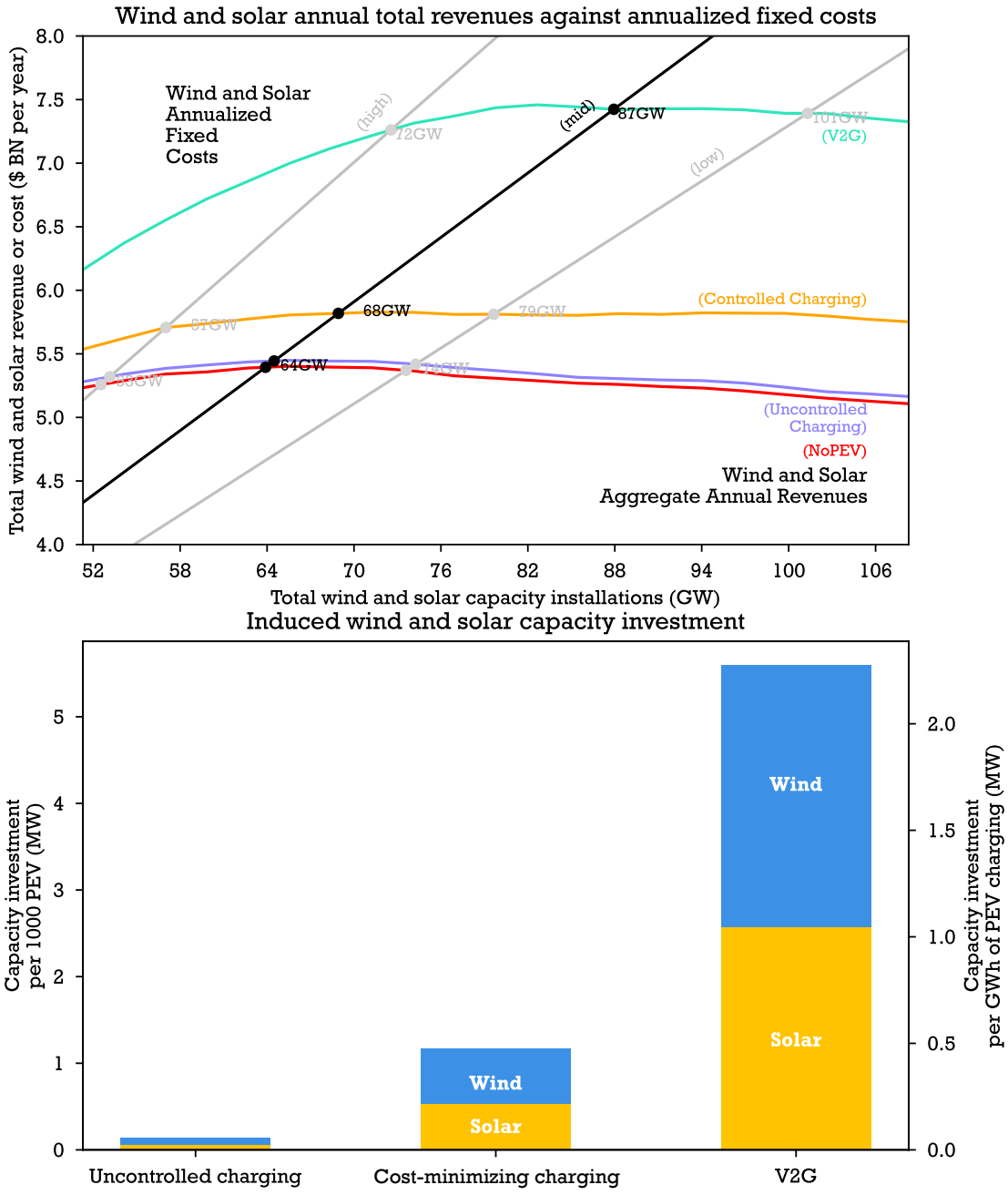


Figure 7: Effect of PEV charging load on the economics of wind and solar capacity investment. Top panel: Total revenues and total annualized fixed costs for solar and wind generators, by PEV and PEV charging intervention scenarios and by wind and solar fixed cost scenarios. **All results in this figure are run with 20% PEV penetration.** All other parameters are the same. Note: (high): conservative fixed cost scenario, (mid): base case fixed cost scenario, (low): optimistic fixed cost scenario. Bottom panel: Wind and solar capacity investment induced by PEV charging interventions, including uncontrolled charging (UC), cost-minimizing charging (CC) and vehicle-to-grid (V2G), relative to the NoPEV baseline scenario. The currency unit is 2024 USD. $ BN is short for billion USD. Further detailed methods are described in the method section.

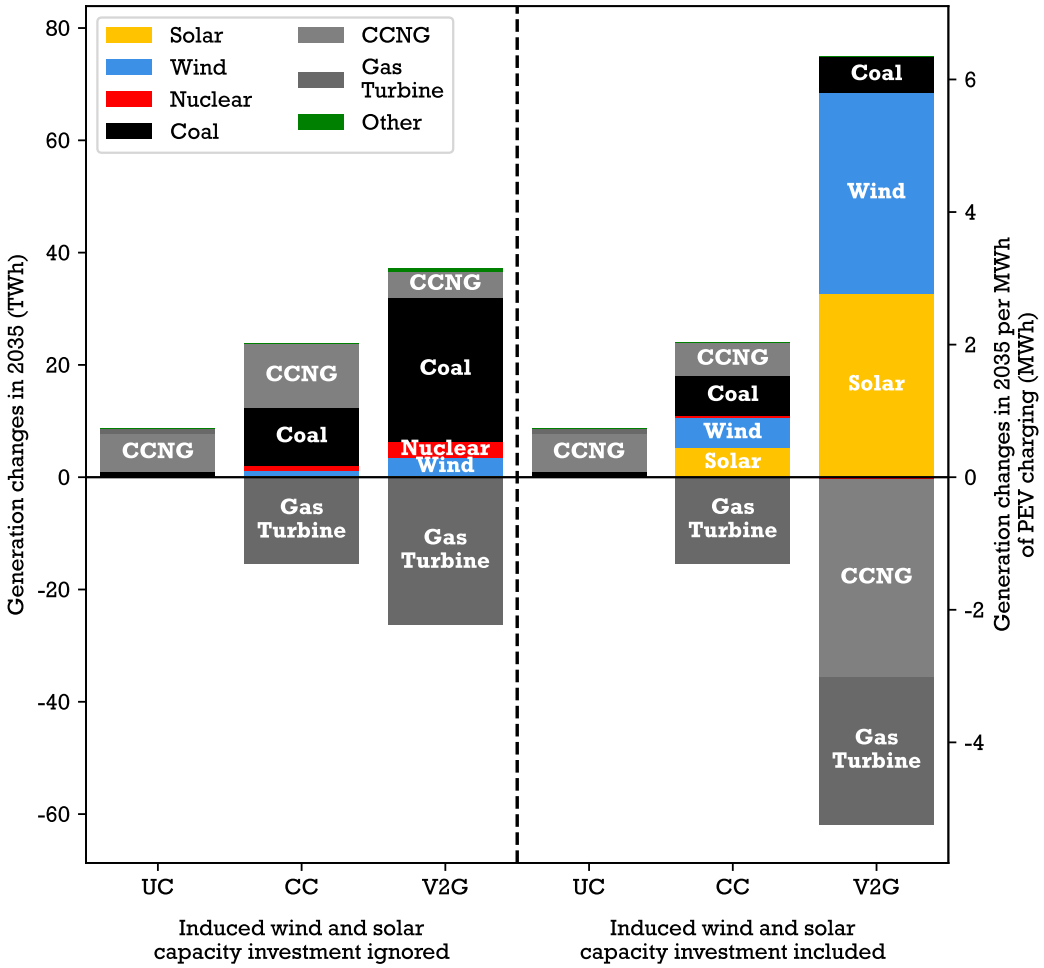


Figure 8: Effect of PEV charging load on power generation. Changes in annual generation by fuel type, relative to the NoPEV case, for each PEV charging scenario when ignoring versus including induced wind and solar capacity investment. **All results in this figure are run with 20% PEV penetration.** All other parameters are the same. When accounting for induced wind and solar investment, wind and solar capacity and therefore generation vary across PEV charging scenarios. 'CCNG' fuel type includes combined cycle natural gas generators. 'Other' fuel types include biomass, fossil waste, fuel cell, hydro, landfill gas, municipal solid waste, non-fossil waste, and oil or gas steam.

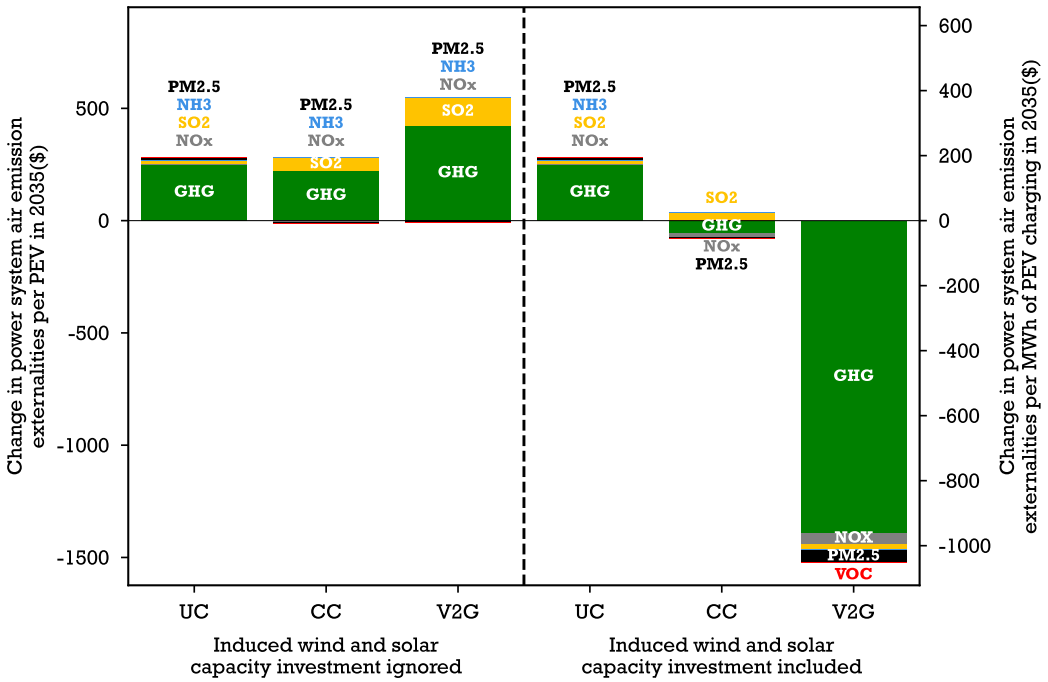


Figure 9: Effect of PEV charging on power system air emission externalities. Change in total power system air emission externalities per PEV and per MWh of PEV charging in 2035, relative to the NoPEV scenario, under each PEV charging scenario when ignoring versus including induced wind and solar capacity investment. The 'ignored' scenarios use generation portfolios given by PJM's grid planning study for 2035 [24]. The 'included' scenarios consider wind and solar capacity at maximum profitable capacity, as described in Method and Materials.

3.4. Wind and solar capacity buildouts

To test the sensitivity of our results on the assumed fixed wind-to-solar capacity ratio, we run a high solar scenario, where solar capacity is increased by 10% and wind reduced by 10% compared with the base case, and a high wind scenario, where wind capacity is increased by 10% and solar reduced by 10% compared with the base case. The comparison with base case shows that while results are sensitive to wind and solar generation profiles, the conclusion still stands that PEVs under V2G can induce wind and solar capacity expansion, reduce overall power grid system costs and overall power grid emission externalities despite PEV charging.

3.4.1. High solar scenario

Shown in Figure 10, with more solar and less wind, the total wind and solar capacity investment induced by V2G changes notably, but capacity investment induction benefits persists and are even higher than the base case. Under a high solar scenario, V2G increases the maximum profitable capacity of wind and solar capacity by 18 GW (a 26% increase) for a combined wind and solar capacity of 70 GW with no PEVs. The increases are 20% higher than under the base case: 15 GW (a 23% increase) increase for a combined capacity with no PEVs of 64 GW.

As a result of higher induced wind and solar capacity investment, the wind and solar generation changes induced by V2G under the high battery scenario are also higher than in the base case (shown in Figure 11). When induced capacity investment is considered, wind and solar generation increases (60 TWh) are 25% higher than under the base case (45 TWh).

When ignoring induced wind and solar capacity investment, total system costs under V2G are 5.5% lower than without PEVs (a $360 per PEV per year reduction). When accounting for induced wind and solar capacity investment, total system costs under V2G are 16% lower than without PEVs (a $1000 per PEV per year reduction). The cost reduction per PEV per year is 14% higher than in the base case (a $880 per PEV per year reduction).

Though results indicate the magnitude of emission externality reduction benefits is quite sensitive to wind and solar generation profiles, the benefits persist to be significant (shown in Figure 12). With higher solar capacity and lower wind capacity, total air emission externalities are reduced by $2300, 4.5% higher compared with the base case.

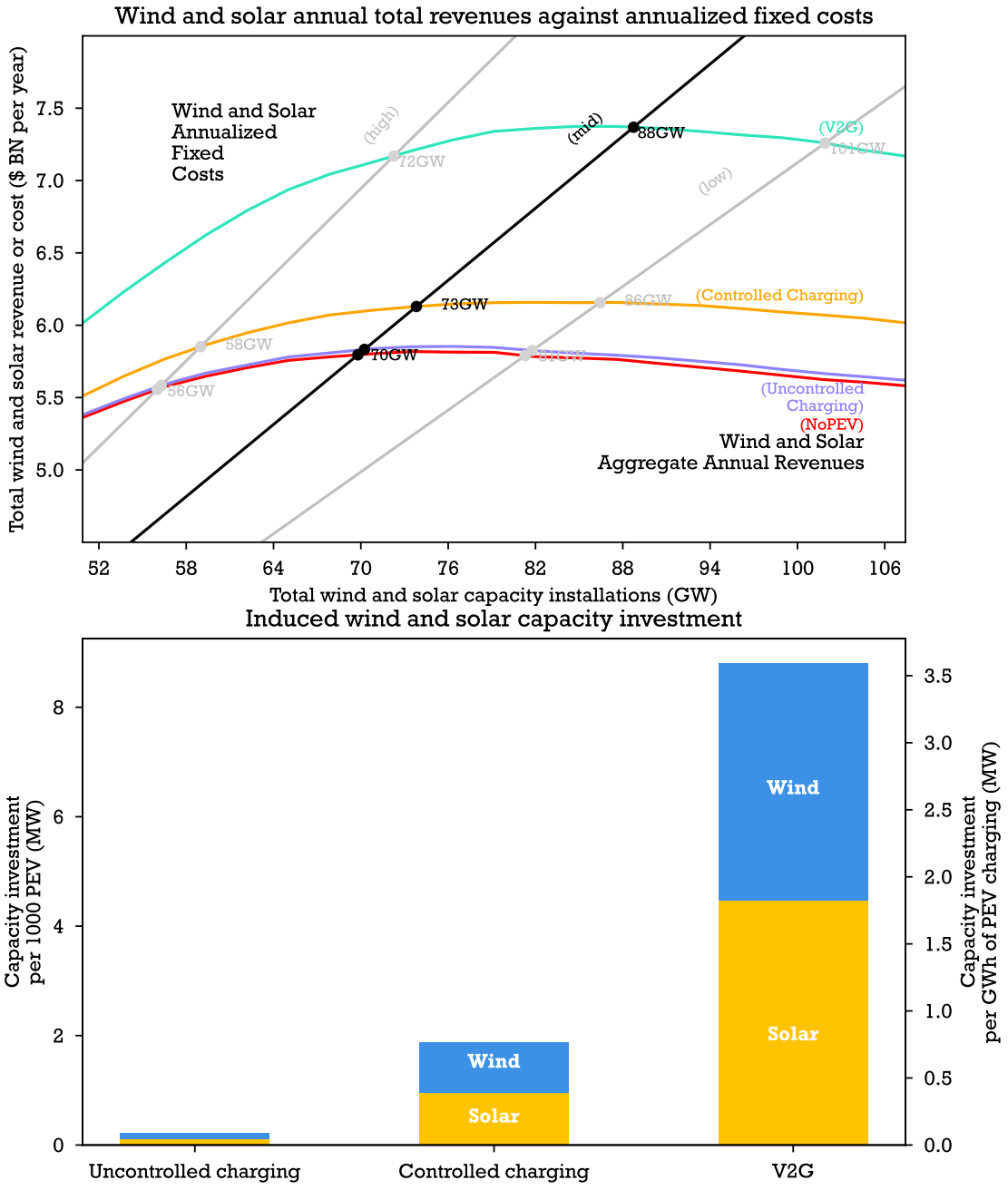


Figure 10: Effect of PEV charging load on the economics of wind and solar capacity investment. Top panel: Total revenues and total annualized fixed costs for solar and wind generators, by PEV and PEV charging intervention scenarios and by wind and solar fixed cost scenarios. **All results in this figure are run with additional solar capacity and lower wind capacity.** All other parameters are the same. Note: (high): conservative fixed cost scenario, (mid): base case fixed cost scenario, (low): optimistic fixed cost scenario. Bottom panel: Wind and solar capacity investment induced by PEV charging interventions, including uncontrolled charging (UC), cost-minimizing charging (CC) and vehicle-to-grid (V2G), relative to the NoPEV baseline scenario. The currency unit is 2024 USD. $ BN is short for billion USD. Further detailed methods are described in the method section.

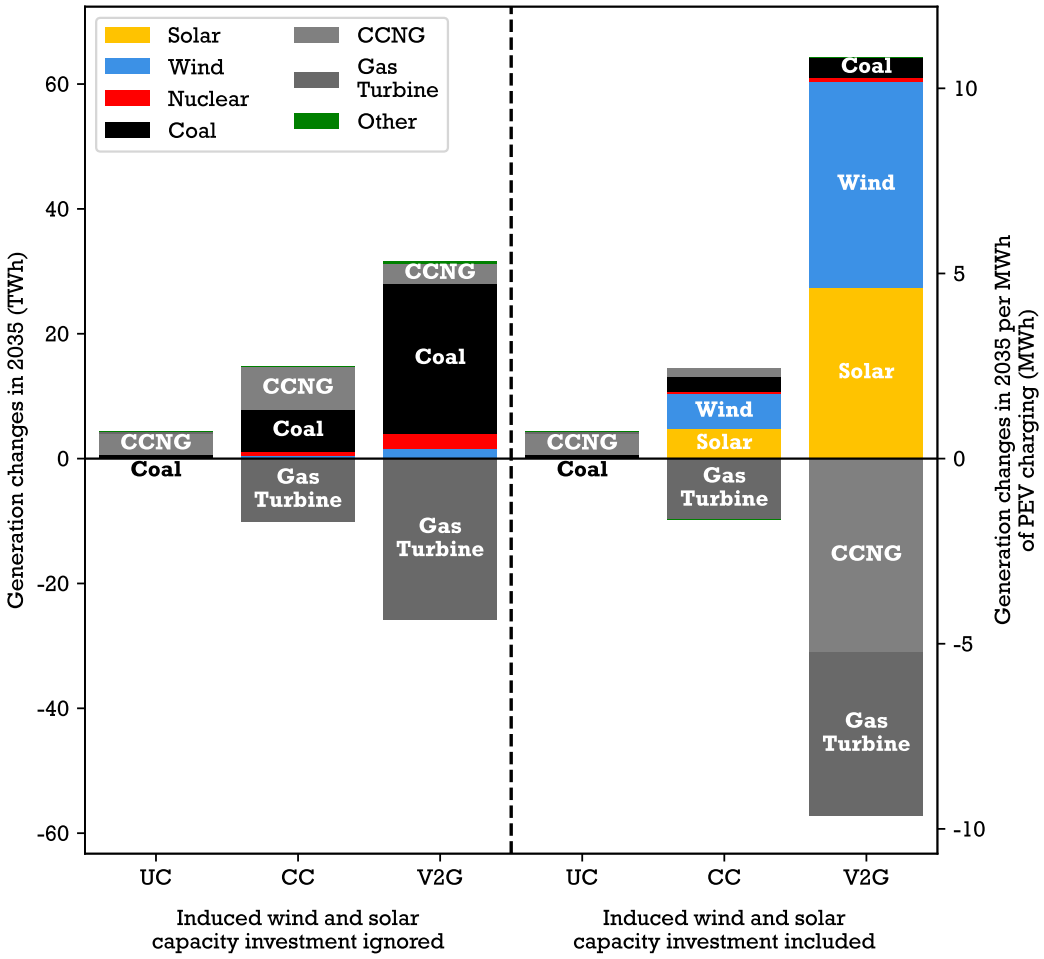


Figure 11: Effect of PEV charging load on power generation. Changes in annual generation by fuel type, relative to the NoPEV case, for each PEV charging scenario when ignoring versus including induced wind and solar capacity investment. **All results in this figure are run with additional solar capacity and lower wind capacity.** All other parameters are the same. When accounting for induced wind and solar investment, wind and solar capacity and therefore generation vary across PEV charging scenarios. 'CCNG' fuel type includes combined cycle natural gas generators. 'Other' fuel types include biomass, fossil waste, fuel cell, hydro, landfill gas, municipal solid waste, non-fossil waste, and oil or gas steam.

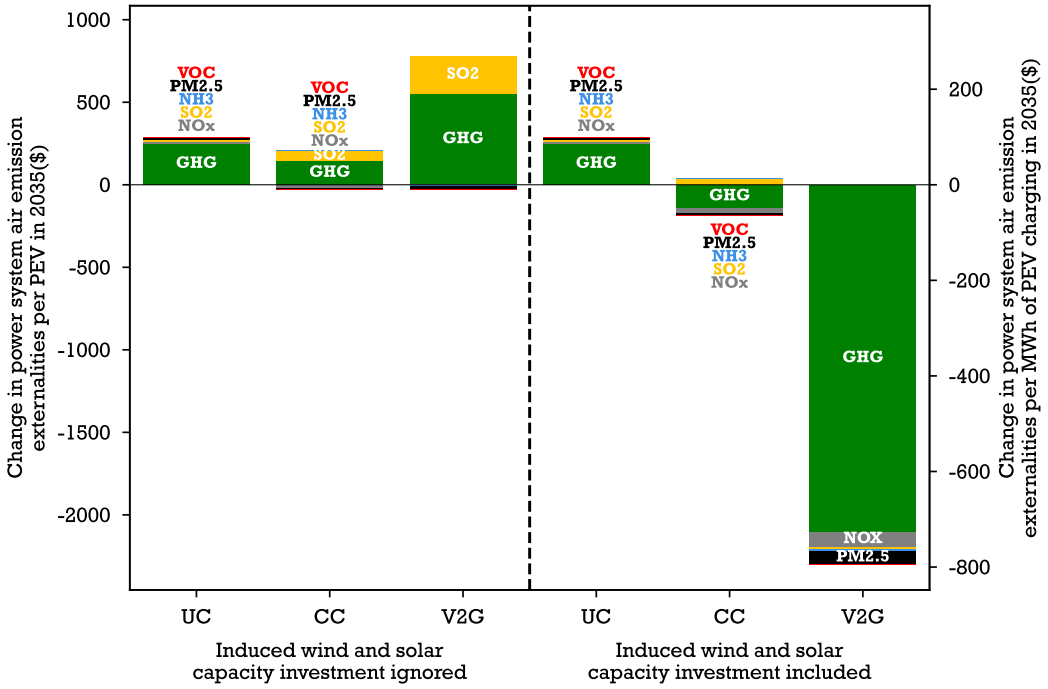


Figure 12: Effect of PEV charging on power system air emission externalities. Change in total power system air emission externalities per PEV and per MWh of PEV charging in 2035, relative to the NoPEV scenario, under each PEV charging scenario when ignoring versus including induced wind and solar capacity investment. The 'ignored' scenarios use generation portfolios given by PJM's grid planning study for 2035 [24]. The 'included' scenarios consider wind and solar capacity at maximum profitable capacity, as described in Method and Materials. **All results in this figure are run with additional solar capacity and lower wind capacity.**

3.4.2. High wind scenario

Shown in Figure 13, with more wind and less solar, the total wind and solar capacity investment induced by V2G changes notably, but capacity investment induction benefits persist and are even higher than the base case. Under a high wind scenario, V2G increases the maximum profitable capacity of wind and solar capacity by 17 GW (a 24% increase) for a combined wind and solar capacity of 71 GW with no PEVs. The increases are 13% higher than under the base case: 15 GW (a 23% increase) increase for a combined capacity with no PEVs of 64 GW.

As a result of higher induced wind and solar capacity investment, the wind and solar generation changes induced by V2G under the high battery scenario are also higher than in the base case (shown in Figure 14). When induced capacity investment is considered, wind and solar generation increases (48 TWh) are 6.7% higher than under the base case (45 TWh).

When ignoring induced wind and solar capacity investment, total system costs under V2G are 5.5% lower than without PEVs (a $360 per PEV per year reduction). When accounting for induced wind and solar capacity investment, total system costs under V2G are 16% lower than without PEVs (a $1000 per PEV per year reduction). The cost reduction per PEV per year which is 14% higher than in the base case (a $880 per PEV per year reduction).

Shown in Figure 15). With higher solar capacity and lower wind capacity, total air emission externalities are reduced by $2300, 4% higher compared with the base case.

The two sets of sensitivity analysis results show that the magnitude of wind and solar capacity investment can be sensitive to wind and solar capacity buildout. As a result of different induced wind and solar capacity investments, system cost reduction benefits and emission reduction benefits can both be sensitive. However, in both sensitivity cases, all V2G benefits, including induced wind and solar capacity investment, system cost reduction benefits and emission reduction benefits, all persist and are higher than in the base case.

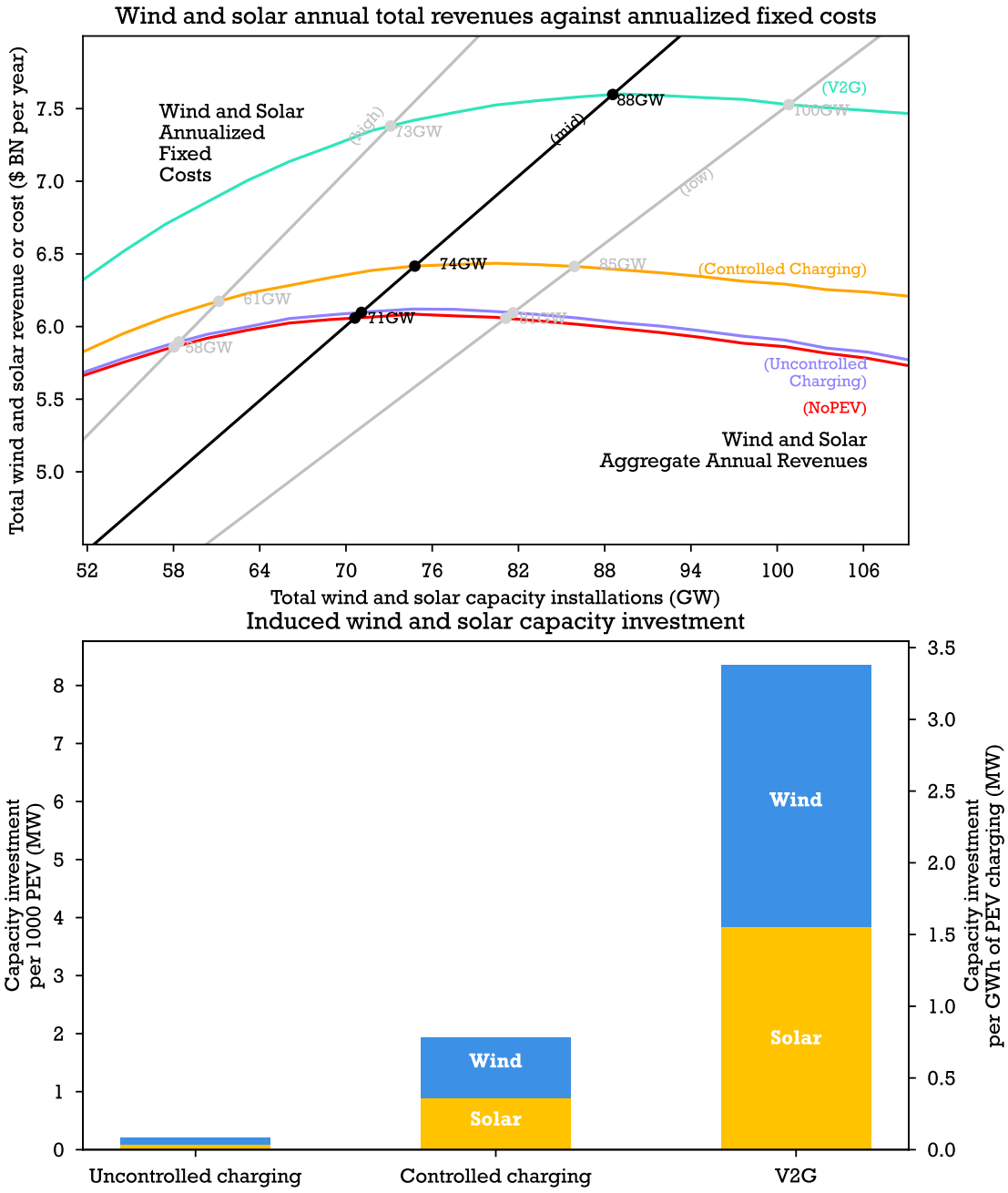


Figure 13: Effect of PEV charging load on the economics of wind and solar capacity investment. Top panel: Total revenues and total annualized fixed costs for solar and wind generators, by PEV and PEV charging intervention scenarios and by wind and solar fixed cost scenarios. **All results in this figure are run with additional wind capacity and lower solar capacity.** All other parameters are the same. Note: (high): conservative fixed cost scenario, (mid): base case fixed cost scenario, (low): optimistic fixed cost scenario. Bottom panel: Wind and solar capacity investment induced by PEV charging interventions, including uncontrolled charging (UC), cost-minimizing charging (CC) and vehicle-to-grid (V2G), relative to the NoPEV baseline scenario. The currency unit is 2024 USD. $ BN is short for billion USD. Further detailed methods are described in the method section.

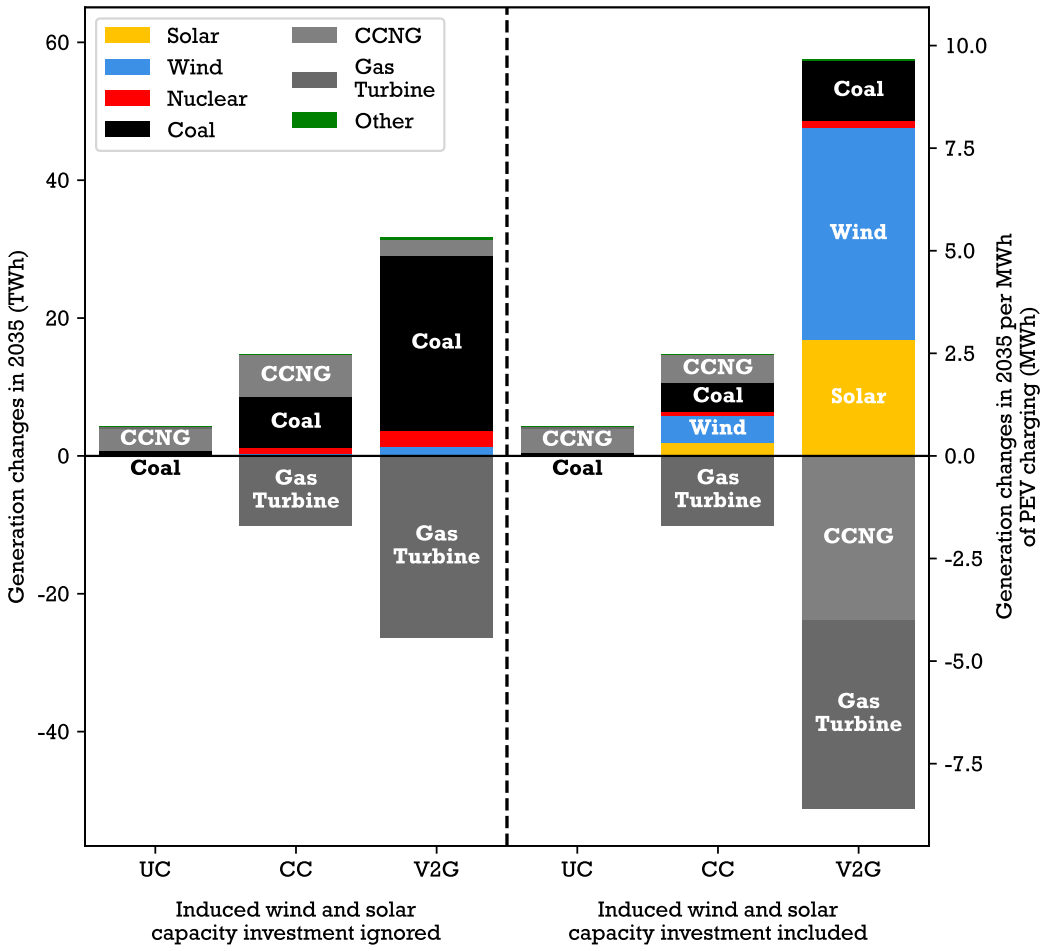


Figure 14: Effect of PEV charging load on power generation. Changes in annual generation by fuel type, relative to the NoPEV case, for each PEV charging scenario when ignoring versus including induced wind and solar capacity investment. **All results in this figure are run with additional wind capacity and lower solar capacity.** All other parameters are the same. When accounting for induced wind and solar investment, wind and solar capacity and therefore generation vary across PEV charging scenarios. 'CCNG' fuel type includes combined cycle natural gas generators. 'Other' fuel types include biomass, fossil waste, fuel cell, hydro, landfill gas, municipal solid waste, non-fossil waste, and oil or gas steam.

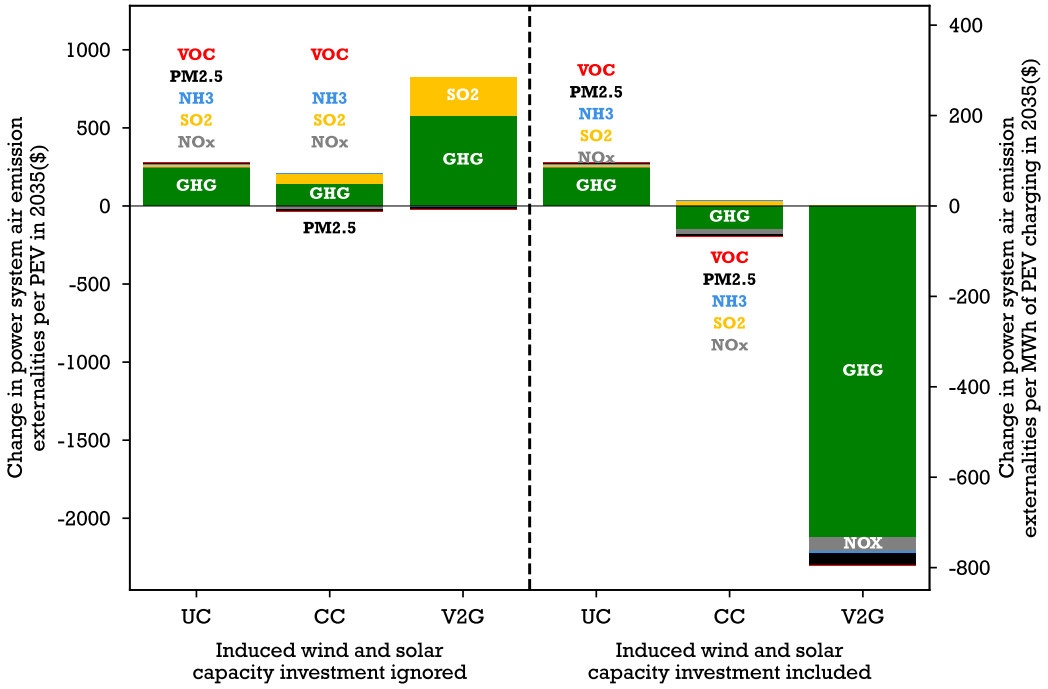


Figure 15: Effect of PEV charging on power system air emission externalities. Change in total power system air emission externalities per PEV and per MWh of PEV charging in 2035, relative to the NoPEV scenario, under each PEV charging scenario when ignoring versus including induced wind and solar capacity investment. The 'ignored' scenarios use generation portfolios given by PJM's grid planning study for 2035 [24]. The 'included' scenarios consider wind and solar capacity at maximum profitable capacity, as described in Method and Materials. **All results in this figure are run with additional solar capacity and lower wind capacity.**

4. Methods

4.1. Variable renewable energy cost estimation

We use cost modeling results from National Renewable Energy Laboratory's Annual Technology Baseline (ATB) database to assess fixed costs of solar and wind generators [25]. 2035 Conservative, Moderate, and Advanced scenarios in ATB correspond to Conservative, Base case, and Optimistic scenarios in our study. Annualized capital costs are calculated with an interest rate of 5% and a capital recovery term of 30 years. The main results reported in the manuscript are based on the Base case scenario. Induced wind and solar capacity is also reported for Conservative and Advanced scenarios. The costs of three scenarios are shown in Table 2.

Table 2: Capital expenditures and fixed O&M costs of wind and power sources in 2024 USD, under different cost scenarios [25]

Technology		Optimistic	Base case	Conservative
On-shore wind	Capital expenditures (USD/kW)	1034	1093	1231
	Annual O&M (USD/kW)	21.6	26.1	28.1
Off-shore wind	Capital expenditures (USD/kW)	2397	2709	3414
	Annual O&M (USD/kW)	75.1	84.5	104.8
Solar	Capital expenditures (USD/kW)	632	829	1101
	Annual O&M (USD/kW)	13.1	15.5	18.9

4.2. PJM System Topography

The original modeling of the PJM Interconnection as 5 transmission constrained regions (TCR) was developed in Lueken et al. 2014 and Weis et al. 2014 [12, 26], which was later updated by Bruchon et al. 2024 [27]. The TCRs and transmission interfaces connecting TCRs are shown in Figure 16. Transmission lines are aggregated into 5 inter-regional transmission interfaces, shown in Figure 17. Transmission capacity of each interfaces are extracted from PJM website (PJM Data Miner).

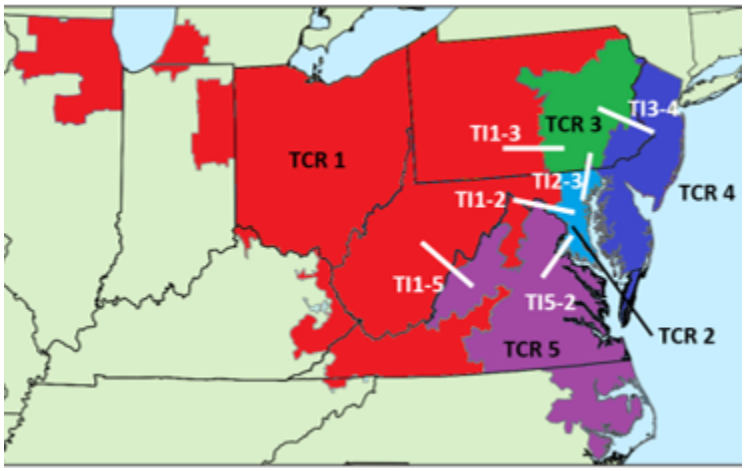


Figure 16: Map of Transmission Constrained Regions (TCRs) and Transmission Interconnections (TIs).

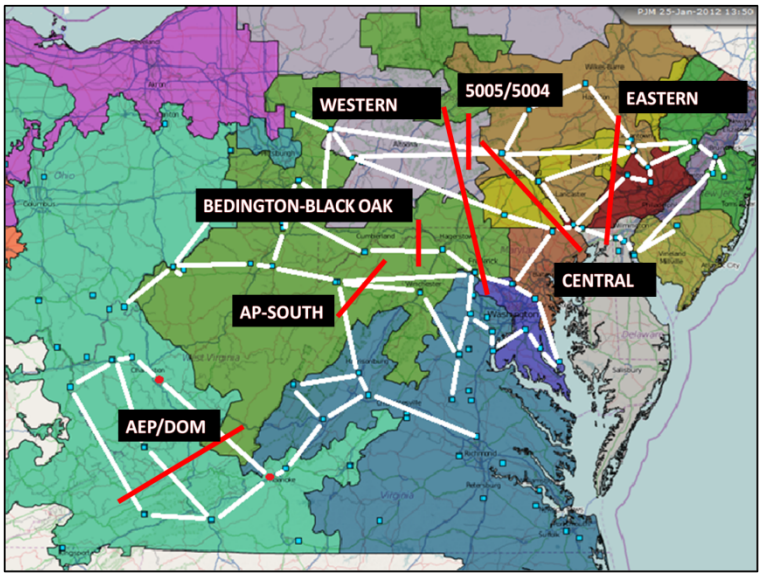


Figure 17: Map of PJM 500kV transmission lines (white lines) and transmission interfaces (red lines). Most interfaces contain multiple 500kV lines. The map illustrates model representation of PJM in Bruchon et al. 2024.

4.3. Power system model formulation

We in this study updated and adapted the unit commitment economic dispatch model formulation of Weis. et al. 2016 and Bruchon et al. 2024 to enable V2G functionalities [27, 28]. The mixed integer optimization problem is formulated as follows in Table 5 and Table 4:

This study models two reserve products: regulation reserve (5min) and spinning reserve (10min). For the calculation of these requirements, we adopt the parameters developed by the National Renewable Energy Laboratory (NREL) ReEDS model [29]. The reserve provision costs account for variable costs incurred by degraded heat rate and other factors, and we adopt the parameters used by NREL's ReEDS model and Craig et al. 2017 (seen in Table tb:rescost) [29, 30].

Table 3: Nomenclature: sets, decision variables, and input parameters.The nomenclature is for Table 4. The problem formulation describes the unit commitment economic dispatch model that simulates hourly simulation of PJM's power system for one year.

Label	Type	Description
$\mathcal{I}$	Set	Generating units
$\mathcal{K}$	Set	Storage units
$\mathcal{R}$	Set	Transmission constraint regions (TCRs)
$\mathcal{T}$	Set	Timesteps
$\mathcal{V}$	Set	Plug-in electric vehicle schedule groups
$c_{v,r,t}^{\text{VEH}}$	Variable	Charge level (MWh) of vehicle schedule group v in TCR r at time t
$c_{k,t}^{\text{STR}}$	Variable	Charge level (MWh) of storage unit k at time t
$p_{i,t}^{\text{GEN}}$	Variable	Power generated by unit i at time t
$p_{r,t}^{\text{SGEN}}$	Variable	Power generated by solar PV generators in TCR r at time t
$p_{r,t}^{\text{WGEN}}$	Variable	Power generated by wind generators in TCR r at time t
$p_{k,t}^{\text{STRD}}$	Variable	Power discharged (+) by storage unit k at time t
$p_{k,t}^{\text{STRC}}$	Variable	Power charged (+) by storage unit k at time t
$p_{r,r',t}^{\text{RR}}$	Variable	Power imported (+) from TCR r' to TCR $r(r \neq r')$ at time t
$p_{v,r,t}^{\text{VR}}$	Variable	Power charged (+) by vehicle schedule group v in TCR r at time t
$p_{v,r,t}^{\text{DR}}$	Variable	Power discharged (+) by vehicle schedule group v in TCR r at time t
$a_{i,t}^{\text{GEN}}$	Variable	Reserve provided by generator unit i at time t
$a_{k,t}^{\text{STR}}$	Variable	Reserve provided by storage unit k at time t
$a_{v,r,t}^{\text{VR}}$	Variable	Reserve provided by vehicle schedule group v in TCR r at time t
$a_{i,t}^{\text{GENSP}}$	Variable	Spinning reserve provided by generator unit i at time t
$a_{k,t}^{\text{STRSP}}$	Variable	Spinning reserve provided by storage unit k at time t
$a_{v,r,t}^{\text{VRSP}}$	Variable	Spinning reserve provided by vehicle schedule group v in TCR r at time t
$s_{i,t}^{\text{STARTUP}}$	Variable	Slack variable for startup cost
$u_{i,t}$	Variable	Binary variable that is equal to 1 if unit i is online in period t and 0 otherwise
$A_{v,t}$	Parameter	Availability of vehicle schedule group v to charge at time t (%)
B_v	Parameter	Battery capacity (MWh) of vehicle grouping v
c_k^{STRMAX}	Parameter	Max charge level (MWh) of storage unit k
c_k^{STRMIN}	Parameter	Min charge level (MWh) of storage unit k
C_i^{VARGEN}	Parameter	Variable cost of generating unit i
C_i^{STARTGEN}	Parameter	Startup cost of generating unit i
$p_{r,t}^{\text{SGENMAX}}$	Parameter	Maximum power generated by solar PV generators in TCR r at time t
$p_{r,t}^{\text{WGENMAX}}$	Parameter	Maximum power generated by wind generators in TCR r at time t
$P_{r,t}$	Parameter	Power demand in TCR r at time t
$p_{r,r',t}^{\text{RRMAX}}$	Parameter	Max power flow on interface (r, r') at time t
$M_{v,t}$	Parameter	Miles traveled per car in vehicle schedule group v at time t
$N_{v,r}$	Parameter	Number of vehicles in schedule group v in TCR r
p_i^{GENMIN}	Parameter	Min generation from unit i at time t
p_i^{GENMAX}	Parameter	Max generation from unit i at time t
p_k^{STRMAX}	Parameter	Max discharge rate from storage unit k
R_i	Parameter	Ramp rate limit of unit i
R_v^{MAXCHG}	Parameter	Max charge rate (MW) of vehicle schedule group v
T_i^{UPMIN}	Parameter	Minimum uptime of unit i
T_i^{DTMIN}	Parameter	Minimum downtime of unit i
C_i^{GENRES}	Parameter	Reserve provision cost of unit i
T_i^{UPSTART}	Parameter	Number of timesteps unit i has been online at initial timestep $t = 1$
T_i^{DTSTART}	Parameter	Number of timesteps unit i has been offline at initial timestep $t = 1$
T_v^{DEPART}	Parameter	Timestep at which vehicle schedule group v departs home
η_v^{CHG}	Parameter	Charging and discharging efficiency (%) of vehicle schedule group v
η_k^{STR}	Parameter	Efficiency (%) of storage unit k
η_v^{VEH}	Parameter	Driving efficiency (MWh/mile) of vehicle schedule group v
η^{TR}	Parameter	Transmission efficiency (%)
p_r^{S}	Parameter	Solar PV capacity of region r (MW)
ϕ^{REG}	Parameter	Ratio of load regulation reserve requirement to load (%)
ϕ^{WIND}	Parameter	Ratio of wind regulation reserve requirement to regional wind generation (%)
ϕ^{SOL}	Parameter	Ratio of solar PV regulation reserve requirement to regional solar PV installed capacity (%)
ϕ^{SPIN}	Parameter	Ratio of spinning reserve requirement to load (%)

Table 4: Optimization problem formulation. The problem formulation describes the unit commitment economic dispatch model that simulates hourly simulation of PJM's power system for one year.

$$\text{Minimize } Z = \sum_{t\in\mathcal{T}}\sum_{i\in I_r}\left(C_i^{\text{VARGEN}}p_{i,t}^{\text{GEN}} + s_{i,t}^{\text{STARTUP}} + C_i^{\text{GENRES}}a_{i,t}^{\text{GEN}}\right) + \sum_{t\in\mathcal{T}}\sum_{k\in\mathcal{K}} C_k^{\text{STR}}a_{k,t}^{\text{STR}} + \sum_{t\in\mathcal{T}}\sum_{v\in\mathcal{V}}\sum_{r\in\mathcal{R}} C^{\text{VEH}}a_{v,r,t}^{\text{VEH}}$$

Subject to

Generator constraints:

$$a_{i,t}^{\text{GEN}} \le 1/12 * \left(p_{i,t-1} + R_i u_{i,t} + p_i^{\text{GENMIN}}(u_{i,t} - u_{i,t-1}) - p_{i,t}\right) - a_{i,t}^{\text{GENSP}} \quad \forall i \in \mathcal{I} \ne 1, \forall t \in \mathcal{T} \quad \text{Generator regulation reserve offer constraints} \quad (1)$$

$$a_{i,t}^{\text{GEN}} \le 1/12 * \left(p_i^{\text{GENMAX}} - p_{i,t}\right) - a_{i,t}^{\text{GENSP}} \quad \forall i \in \mathcal{I} \ne 1, \forall t \in \mathcal{T} \quad \text{Generator regulation reserve offer constraints} \quad (2)$$

$$a_{i,t}^{\text{GEN}} \le 1/12 * \left(p_i^{\text{GENMAX}} u_{i,t}\right) - a_{i,t}^{\text{GENSP}} \quad \forall i \in \mathcal{I} \ne 1, \forall t \in \mathcal{T} \quad \text{Generator regulation reserve offer constraints} \quad (3)$$

$$a_{i,t}^{\text{GENSP}} \le 1/6 * \left(p_{i,t-1} + R_i u_{i,t} + p_i^{\text{GENMIN}}(u_{i,t} - u_{i,t-1}) - p_{i,t}\right) - a_{i,t}^{\text{GENSP}} \quad \forall i \in \mathcal{I} \ne 1, \forall t \in \mathcal{T} \quad \text{Generator spinning reserve offer constraints} \quad (4)$$

$$a_{i,t}^{\text{GENSP}} \le 1/6 * \left(p_i^{\text{GENMAX}} - p_{i,t}\right) - a_{i,t}^{\text{GEN}} \quad \forall i \in \mathcal{I} \ne 1, \forall t \in \mathcal{T} \quad \text{Generator spinning reserve offer constraints} \quad (5)$$

$$a_{i,t}^{\text{GENSP}} \le 1/6 * \left(p_i^{\text{GENMAX}} u_{i,t}\right) - a_{i,t}^{\text{GEN}} \quad \forall i \in \mathcal{I} \ne 1, \forall t \in \mathcal{T} \quad \text{Generator spinning reserve offer constraints} \quad (6)$$

$$s_{i,t}^{\text{STARTUP}} \ge \left(u_{i,t} - u_{i,t-1}\right) C_i^{\text{STARTGEN}} \quad \forall i \in \mathcal{I}, \forall t \in \mathcal{T} \quad \text{Slack variable reflects startup decision} \quad (7)$$

$$s_{i,t}^{\text{STARTUP}} \ge 0 \quad \forall i \in \mathcal{I}, \forall t \in \mathcal{T} \quad \text{Slack variable is nonnegative} \quad (8)$$

$$p_i^{\text{GENMIN}} u_{i,t} \le p_{i,t} \le p_i^{\text{GENMAX}} u_{i,t} \quad \forall i \in \mathcal{I}, \forall t \in \mathcal{T} \quad \text{Min and max output of online generators} \quad (9)$$

$$p_{i,t}^{\text{GEN}} \le p_{i,t-1}^{\text{GEN}} + R_i u_{i,t-1} + p_i^{\text{GENMIN}}\left(u_{i,t} - u_{i,t-1}\right) \quad \forall i \in \mathcal{I}, \forall t \in \mathcal{T} \quad \text{Ramp rate limit} \quad (10)$$

$$p_{i,t-1}^{\text{GEN}} \le p_{i,t}^{\text{GEN}} + R_i u_{i,t} + p_i^{\text{GENMIN}}\left(u_{i,t-1} - u_{i,t}\right) \quad \forall i \in \mathcal{I}, \forall t \in \mathcal{T} \quad \text{Ramp rate limit} \quad (11)$$

$$\sum_{t=2}^{T_i^{\text{UPMIN}} - T_i^{\text{UPSTART}}} \left(1 - u_{i,t}\right) = 0 \quad \forall i \in \mathcal{I} \quad \text{Minimum uptime (first timesteps)} \quad (12)$$

$$\sum_{t'=t}^{t+T_i^{\text{UPMIN}}-1} u_{i,t'} \ge T_i^{\text{UPMIN}}\left(u_{i,t} - u_{i,t-1}\right) \quad \forall i \in \mathcal{I}, \forall t : T_i^{\text{UPMIN}} - T_i^{\text{UPSTART}} + 1 \le t \le |\mathcal{T}| - T_i^{\text{UPMIN}} + 1 \quad \text{Minimum uptime (middle timesteps)} \quad (13)$$

$$\sum_{t=t}^{T} u_{i,t'} \ge (T - t)\left(u_{i,t} - u_{i,t-1}\right) \quad \forall i \in \mathcal{I}, \forall t \in |\mathcal{T}| - T_i^{\text{UPMIN}} + 2 \ldots \quad \text{Minimum uptime (final timesteps)} \quad (14)$$

$$\sum_{t=2}^{T_i^{\text{DTMIN}} - T_i^{\text{DTSTART}}} u_{i,t} = 0 \quad \forall i \in \mathcal{I} \quad \text{Minimum downtime (first timesteps)} \quad (15)$$

$$\sum_{t'=t}^{t+T_i^{\text{DTMIN}}-1} 1 - u_{i,t'} \ge T_i^{\text{DTMIN}}\left(u_{i,t-1} - u_{i,t}\right) \quad \forall i \in \mathcal{I}, \forall t : T_i^{\text{DTSTART}} + 1 \le t \le |\mathcal{T}| - T_i^{\text{DTSTART}} + 1 \quad \text{Minimum downtime (middle timesteps)} \quad (16)$$

$$\sum_{t'=t}^{T} 1 - u_{i,t'} \ge (|\mathcal{T}| - t)\left(u_{i,t-1} - u_{i,t}\right) \quad \forall i \in \mathcal{I}, \forall t : |\mathcal{T}| - T_i^{\text{DTSTART}} + 2 \le t \le |\mathcal{T}| \quad \text{Minimum downtime (final timesteps)} \quad (17)$$

Table 5: Optimization problem formulation (continued).

$$\text{Minimize } Z = \sum_{t\in\mathcal{T}}\sum_{i\in I_r}\left(C_i^{\text{VARGEN}}p_{i,t}^{\text{GEN}} + s_{i,t}^{\text{STARTUP}} + C_i^{\text{GENRES}}a_{i,t}^{\text{GEN}}\right) + \sum_{t\in\mathcal{T}}\sum_{k\in\mathcal{K}} C_k^{\text{STR}}a_{k,t}^{\text{STR}} + \sum_{t\in\mathcal{T}}\sum_{v\in\mathcal{V}}\sum_{r\in\mathcal{R}} C^{\text{VEH}}a_{v,r,t}^{\text{VEH}}$$

Subject to

System constraints:

$$P_{r,t} = \sum_{i\in\mathcal{I}_r} p_{i,t}^{\text{GEN}} + \sum_{k\in\mathcal{K}_r} p_{i,t}^{\text{STRD}} - \sum_{k\in\mathcal{K}_r} p_{i,t}^{\text{STRC}} - \sum_{r'\in\mathcal{R}\neq r}(p_{r',r,t}^{\text{RR}}) + \sum_{r'\in\mathcal{R}\neq r}(p_{r,r',t}^{\text{RR}}\eta^{\text{TR}}) + p_{r,t}^{\text{SGEN}} + p_{r,t}^{\text{WGEN}} - \sum_{v\in\mathcal{V}_r} p_{v,r,t}^{\text{VR}} + \sum_{v\in\mathcal{V}_r} p_{v,r,t}^{\text{DR}} \quad \forall r\in\mathcal{R}, t\in\mathcal{T} \quad \text{Demand must equal supply} \quad (18)$$

$$-p_{r,r',t}^{\text{RRMAX}} \le p_{r,r',t}^{\text{RR}} \le p_{r,r',t}^{\text{RRMAX}} \quad \forall r\in\mathcal{R}, r'\in\mathcal{R}\neq r, t\in\mathcal{T} \quad \text{Inter-region power flow limits} \quad (19)$$

$$0 \le p_{r,t}^{\text{SGEN}} \le p_{r,t}^{\text{SGENMAX}} \quad \forall r\in\mathcal{R}, t\in\mathcal{T} \quad \text{Regional solar PV output limits} \quad (20)$$

$$0 \le p_{r,t}^{\text{WGEN}} \le p_{r,t}^{\text{WGENMAX}} \quad \forall r\in\mathcal{R}, t\in\mathcal{T} \quad \text{Regional wind generator output limits} \quad (21)$$

$$\phi^{SPIN} * P_{r,t} = \sum_{i\in\mathcal{I}_r} a_{i,t}^{\text{GENSP}} + \sum_{k\in\mathcal{K}_r} a_{k,t}^{\text{STRSP}} + \sum_{v\in\mathcal{V}_r} a_{v,r,t}^{\text{VRSP}} \quad \forall r\in\mathcal{R}, t\in\mathcal{T} \quad \text{Regional spinning reserve requirement must be met} \quad (22)$$

$$\phi^{REG} * P_{r,t} + \phi^{\text{WIND}} * p_{r,t}^{\text{WGEN}} + \phi^{\text{SOL}} * p^{\text{S}} = \sum_{i\in\mathcal{I}_r} a_{i,t}^{\text{GEN}} + \sum_{k\in\mathcal{K}_r} a_{k,t}^{\text{STR}} + \sum_{v\in\mathcal{V}_r} a_{v,r,t}^{\text{VR}} \quad \forall r\in\mathcal{R}, t\in\mathcal{T} \quad \text{Regional regulation reserve requirement must be met} \quad (23)$$

Storage constraints:

$$c_{k,t+1}^{\text{STR}} = c_{k,t}^{\text{STR}} + p_{k,t}^{\text{STRC}}\eta^{STR} - p_{k,t}^{\text{STRD}}/\eta^{STR} \quad \forall k\in\mathcal{K}, \forall t\in\mathcal{T} \quad \text{Storage state of charge} \quad (24)$$

$$c_k^{\text{STRMIN}} \le c_{k,t}^{\text{STR}} \le c_k^{\text{STRMAX}} \quad \forall k\in\mathcal{K}, \forall t\in\mathcal{T} \quad \text{Storage unit capacity} \quad (25)$$

$$0 \le p_{k,t}^{\text{STRD}}, p_{k,t}^{\text{STRC}} \le p_k^{\text{STRMAX}} \quad \forall k\in\mathcal{K}, \forall t\in\mathcal{T} \quad \text{Max charge and discharge of storage units} \quad (26)$$

$$a_{k,t}^{\text{STRSP}} \le p_k^{\text{STRMAX}} - p_{k,t}^{\text{STRD}} + p_{k,t}^{\text{STRC}} - a_{k,t}^{\text{STR}} \quad \forall k\in\mathcal{K}, \forall t\in\mathcal{T} \quad \text{Max regulation and spinning reserve offer of storage units} \quad (27)$$

$$a_{k,t}^{\text{STRSP}} \le c_{k,t}^{\text{STR}} - a_{k,t}^{\text{STR}} \quad \forall k\in\mathcal{K}, \forall t\in\mathcal{T} \quad \text{Max regulation and spinning reserve offer of storage units} \quad (28)$$

PEV constraints:

$$c_{v,r,t+1}^{\text{VEH}} = c_{v,r,t}^{\text{CHG}} - p_{v,r,t}^{\text{VR}}\eta_v^{\text{VEH}} - N_{v,r}M_{v,t}\eta_v^{\text{VEH}} \quad \forall v\in\mathcal{V}, \forall r\in\mathcal{R}, \forall t\in\mathcal{T} \quad \text{PEV state of charge} \quad (29)$$

$$10\%N_{v,r}B_v \le c_{v,r,t}^{\text{VEH}} \le 90\%N_{v,r}B_v \quad \forall v\in\mathcal{V}, \forall r\in\mathcal{R}, \forall t\in\mathcal{T} \quad \text{PEV battery capacity} \quad (30)$$

$$c_{v,r,t}^{\text{VEH}} = 90\%N_{v,r}B_v \quad \forall v\in\mathcal{V}, \forall r\in\mathcal{R}, \forall t = T_v^{\text{DEPART}} \quad \text{PEVs fully charged when departing home} \quad (31)$$

$$c_{v,r,t+1}^{\text{VEH}} = c_{v,r,t}^{\text{CHG}} - p_{v,r,t}^{\text{VR}}/\eta_v^{\text{CHG}} + p_{v,r,t}^{\text{DR}} * \eta_v^{\text{CHG}}N_{v,r}M_{v,t}\eta_v^{\text{VEH}} \quad \forall v\in\mathcal{V}, \forall r\in\mathcal{R}, \forall t\in\mathcal{T} \quad \text{PEV state of charge} \quad (32)$$

$$0 \le p_{v,r,t}^{\text{VR}}, p_{v,r,t}^{\text{DR}} \le N_{v,r}A_{v,t}R_v^{\text{MAXCHG}} \quad \forall v\in\mathcal{V}, \forall r\in\mathcal{R}, \forall t\in\mathcal{T} \quad \text{PEV charge rate limit} \quad (33)$$

$$0 \le c_{v,r,t}^{\text{VEH}} \le N_{v,r}B_v \quad \forall v\in\mathcal{V}, \forall r\in\mathcal{R}, \forall t\in\mathcal{T} \quad \text{PEV battery capacity} \quad (34)$$

$$a_{v,r,t}^{\text{VRSP}} \le N_{v,r}A_{v,t}R_v^{\text{MAXCHG}} - p_{v,r,t}^{\text{DR}} + p_{v,r,t}^{\text{VR}} - a_{v,r,t}^{\text{VR}} \quad \forall r\in\mathcal{R}, \forall v\in\mathcal{V} \quad \text{Max regulation and spinning reserve offer of vehicle fleets} \quad (35)$$

$$a_{v,r,t}^{\text{VRSP}} \le c_{v,r,t}^{\text{VEH}} - a_{v,r,t}^{\text{VR}} \quad \forall r\in\mathcal{R}, \forall v\in\mathcal{V}, \forall t\in\mathcal{T} \quad (36)$$

Table 6: Reserve provisional costs of different reserve providers by fuel type or technology type

Fuel and technology type	Coal	Combined Cycle Natural Gas	Gas/Oil steam	Storage	Storage by PEV
Cost($/MWh)	10	6	4	2	2

5. More results

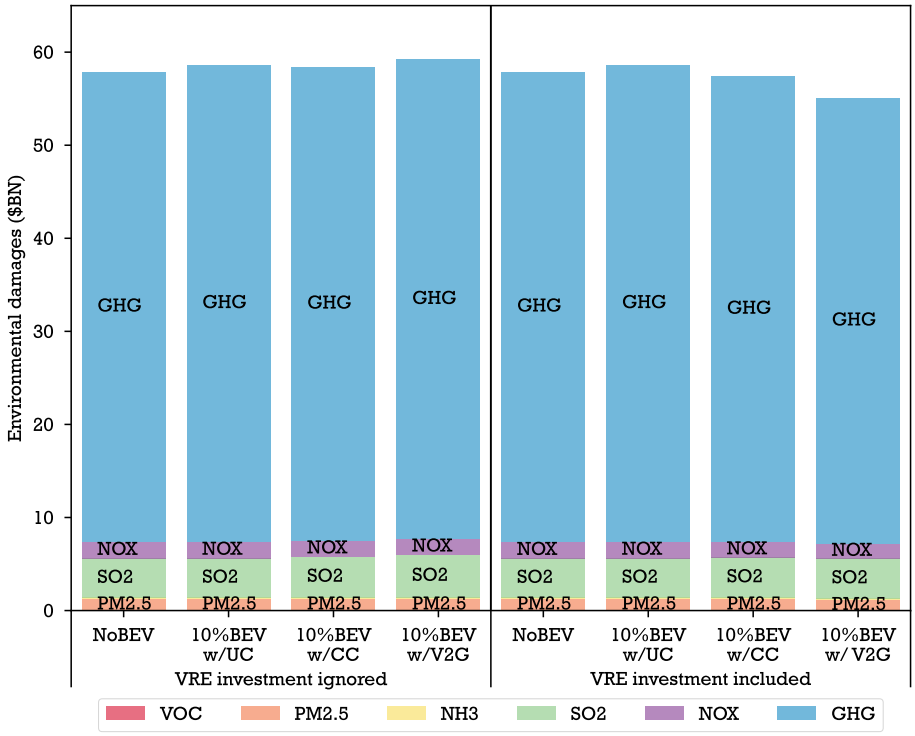


Figure 18: Annual environmental externalities of GHG emissions and pollution, by different PEV and PEV charging intervention scenarios and analysis approaches. Wind and power capacity varies across PEV and PEV charging intervention scenarios in Expansion scenarios, as PEV and PEV charging intervention affects the maximum profitable wind and power capacity installation. Environmental externalities for GHG emissions are calculated with social cost of carbon of \$204/ton CO_2e in 2023, published by US Environment Protection Agency[31]. The results with a lower cost of carbon of \$51/ton CO_2e can be found in SI. The AP3 model is used to calculate those of pollutants.

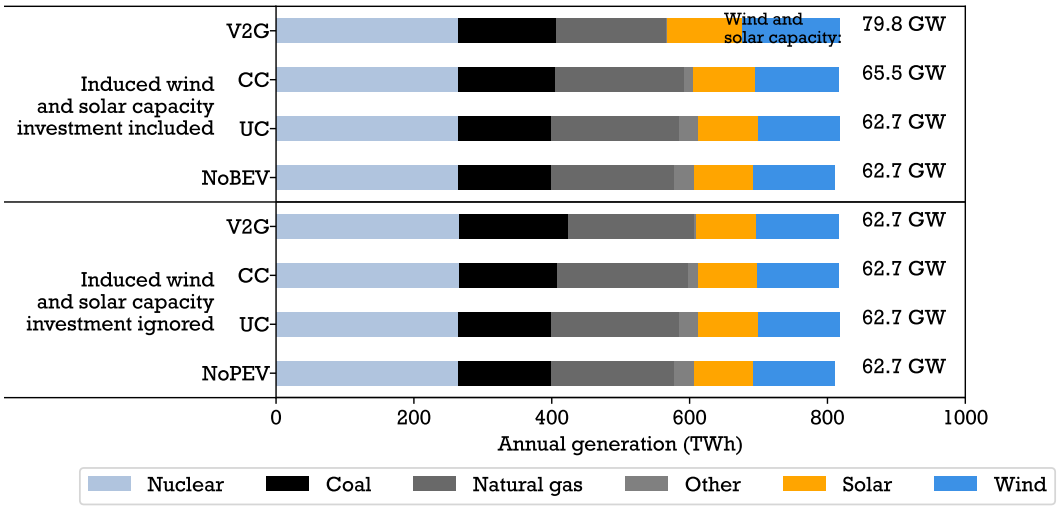


Figure 19: Annual generation of different fuel types, by different PEV and PEV charging intervention scenarios and analysis approaches. Wind and solar capacity varies across PEV and PEV charging intervention scenarios in wind and solar capacity investment scenarios, as PEV and PEV charging interventions affect the maximum profitable wind and solar capacity installations. 'Natural gas' fuel type includes combined cycle natural gas generators and gas turbine generators. 'Other' fuel types include biomass, fossil waste, fuel cell, hydro, landfill gas, municipal solid waste, non-fossil waste, and oil or gas steam.

Table 7: Annual emissions and environmental externalities of greenhouse gases and air pollutants, by different grid intervention scenarios and analysis approaches. wind and power capacity varies across grid intervention scenarios in wind and power scenarios, as PEV charging intervention intervention affects the maximum profitable wind and power capacity installation. Environmental externalities for GHG emissions are calculated with social cost of carbon of \$204/ton CO_2e. The AP3 model is used to calculate those of pollutants. All costs are in 2024 USD.

			Emission Externalities (\$MM)					
			GHG	NOx	SO2	NH3	PM25	VOC
Wind and Solar Capacity Investment	Ignored	NoPEV	50455	1765	4195	165	1208	14
		Uncontrolled charging	51152	1771	4206	182	1246	15
		Cost-minimizing charging	50895	1685	4380	181	1199	13
		V2G	51467	1730	4595	180	1182	13
	Included	NoPEV	50455	1765	4195	165	1208	14
		Uncontrolled charging	51152	1771	4206	182	1246	15
		Cost-minimizing charging	50013	1662	4286	178	1180	13
		V2G	46155	1568	4128	163	1052	12

References

[1] S. P. Holland, M. J. Kotchen, E. T. Mansur, A. J. Yates, Why marginal CO2 emissions are not decreasing for US electricity: Estimates and implications for climate policy, Proceedings of the National Academy of Sciences 119 (8) (2022) e2116632119, publisher: Proceedings of the National Academy of Sciences. doi:10.1073/pnas.2116632119.
URL https://www.pnas.org/doi/abs/10.1073/pnas.2116632119

[2] R. Tu, Y. J. Gai, B. Farooq, D. Posen, M. Hatzopoulou, Electric vehicle charging optimization to minimize marginal greenhouse gas emissions from power generation, Applied Energy 277 (2020) 115517. doi:10.1016/j.apenergy.2020.115517.
URL http://www.sciencedirect.com/science/article/pii/S0306261920310291

[3] J. Chen, F. Wang, X. He, X. Liang, J. Huang, S. Zhang, Y. Wu, Emission mitigation potential from coordinated charging schemes for future private electric vehicles, Applied Energy 308 (2022) 118385. doi:10.1016/j.apenergy.2021.118385.
URL https://www.sciencedirect.com/science/article/pii/S0306261921016238

[4] M. Wang, M. T. Craig, The value of vehicle-to-grid in a decarbonizing California grid, Journal of Power Sources 513 (2021) 230472. doi:10.1016/j.jpowsour.2021.230472.
URL https://www.sciencedirect.com/science/article/pii/S0378775321009757

[5] R. Shi, S. Li, P. Zhang, K. Y. Lee, Integration of renewable energy sources and electric vehicles in V2G network with adjustable robust optimization, Renewable Energy 153 (2020) 1067–1080. doi:10.1016/j.renene.2020.02.027.
URL https://www.sciencedirect.com/science/article/pii/S0960148120302135

[6] N. A. Ryan, J. X. Johnson, G. A. Keoleian, Comparative Assessment of Models and Methods To Calculate Grid Electricity Emissions, Environmental Science & Technology 50 (17) (2016) 8937–8953, publisher: American Chemical Society. doi:10.1021/acs.est.5b05216.
URL https://doi.org/10.1021/acs.est.5b05216

[7] X. Chen, H. Zhang, Z. Xu, C. P. Nielsen, M. B. McElroy, J. Lv, Impacts of fleet types and charging modes for electric vehicles on emissions under different penetrations of wind power, Nature Energy 3 (5) (2018) 413–421, publisher: Nature Publishing Group.

[8] J. Owens, I. Miller, E. Gençer, Can vehicle-to-grid facilitate the transition to low carbon energy systems?, Energy Advances 1 (12) (2022) 984–998, publisher: Royal Society of Chemistry. doi:10.1039/D2YA00204C.
URL https://pubs.rsc.org/en/content/articlelanding/2022/ya/d2ya00204c

[9] P. Gagnon, W. Cole, Planning for the evolution of the electric grid with a long-run marginal emission rate, iScience 25 (3) (2022) 103915. doi:10.1016/j.isci.2022.103915.
URL https://www.sciencedirect.com/science/article/pii/S2589004222001857

[10] T. Brown, D. Schlachtberger, A. Kies, S. Schramm, M. Greiner, Synergies of sector coupling and transmission reinforcement in a cost-optimised, highly renewable European energy system, Energy 160 (2018) 720–739. doi:10.1016/j.energy.2018.06.222.
URL https://www.sciencedirect.com/science/article/pii/S036054421831288X

[11] F. Manríquez, E. Sauma, J. Aguado, S. de la Torre, J. Contreras, The impact of electric vehicle charging schemes in power system expansion planning, Applied Energy 262 (2020) 114527. doi:10.1016/j.apenergy.2020.114527.
URL https://www.sciencedirect.com/science/article/pii/S0306261920300398

[12] A. Weis, P. Jaramillo, J. Michalek, Estimating the potential of controlled plug-in hybrid electric vehicle charging to reduce operational and capacity expansion costs for electric power systems with high wind penetration, Applied Energy 115 (2014) 190–204. doi:10.1016/j.apenergy.2013.10.017.
URL https://www.sciencedirect.com/science/article/pii/S0306261913008374

[13] E. S. Hittinger, I. M. L. Azevedo, Bulk Energy Storage Increases United States Electricity System Emissions, Environmental Science & Technology 49 (5) (2015) 3203–3210, publisher: American Chemical Society. doi:10.1021/es505027p.
URL https://doi.org/10.1021/es505027p

[14] M. Muratori, Impact of uncoordinated plug-in electric vehicle charging on residential power demand, Nature Energy 3 (3) (2018) 193–201. doi:10.1038/s41560-017-0074-z.
URL http://www.nature.com/articles/s41560-017-0074-z

[15] M. E. Kahn, R. K. Vaughn, Green Market Geography: The Spatial Clustering of Hybrid Vehicles and LEED Registered Buildings, The B.E. Journal of Economic Analysis & Policy 9 (2), publisher: De Gruyter (Mar. 2009). doi:10.2202/1935-1682.2030.
URL https://www.degruyter.com/document/doi/10.2202/1935-1682.2030/html

[16] P. R. Brown, F. M. O'Sullivan, Spatial and temporal variation in the value of solar power across United States electricity markets, Renewable and Sustainable Energy Reviews 121 (2020) 109594. doi:10.1016/j.rser.2019.109594.
URL https://www.sciencedirect.com/science/article/pii/S1364032119308020

[17] M. Vanatta, M. T. Craig, B. Rathod, J. Florez, I. Bromley-Dulfano, D. Smith, The costs of replacing coal plant jobs with local instead of distant wind and solar jobs across the United States, iScience 25 (8) (2022) 104817. doi:10.1016/j.isci.2022.104817.

[18] M. Carrión, R. Zárate-Miñano, Operation of renewable-dominated power systems with a significant penetration of plug-in electric vehicles, Energy 90 (2015) 827–835. doi:10.1016/j.energy.2015.07.111.
URL https://www.sciencedirect.com/science/article/pii/S0360544215010063

[19] A. Jenn, K. Clark-Sutton, M. Gallaher, J. Petrusa, Environmental impacts of extreme fast charging, Environmental Research Letters 15 (9) (2020) 094060, publisher: IOP Publishing. doi:10.1088/1748-9326/ab9870.
URL https://dx.doi.org/10.1088/1748-9326/ab9870

[20] A. Weis, J. J. Michalek, P. Jaramillo, R. Lueken, Emissions and Cost Implications of Controlled Electric Vehicle Charging in the U.S. PJM Interconnection, Environmental Science & Technology 49 (9) (2015) 5813–5819. doi:10.1021/es505822f.
URL https://pubs.acs.org/doi/10.1021/es505822f

[21] P. Nunes, M. C. Brito, Displacing natural gas with electric vehicles for grid stabilization, Energy 141 (2017) 87–96. doi:10.1016/j.energy.2017.09.064.
URL https://www.sciencedirect.com/science/article/pii/S0360544217315852

[22] K. E. Forrest, B. Tarroja, L. Zhang, B. Shaffer, S. Samuelsen, Charging a renewable future: The impact of electric vehicle charging intelligence on energy storage requirements to meet renewable portfolio standards, Journal of Power Sources 336 (2016) 63–74. doi:10.1016/j.jpowsour.2016.10.048.
URL https://www.sciencedirect.com/science/article/pii/S0378775316314409

[23] B. Tarroja, L. Zhang, V. Wifvat, B. Shaffer, S. Samuelsen, Assessing the stationary energy storage equivalency of vehicle-to-grid charging battery electric vehicles, Energy 106 (2016) 673–690. doi:10.1016/j.energy.2016.03.094.
URL https://www.sciencedirect.com/science/article/pii/S0360544216303383

[24] PJM, Energy Transition in PJM: Frameworks for Analysis, Tech. rep. (Dec. 2021).
URL https://pjm.com/-/media/committees-groups/committees/mrc/2021/20211215/20211215-item-09-energy-transition-in-pjm-whitepaper.ashx

[25] L. Vimmerstedt, T. Stehly, S. Akar, A. Sekar, B. Mirletz, D. Stright, C. Augustine, P. Beiter, P. Bhaskar, N. Blair, S. Cohen, W. Cole, P. Duffy, D. Feldman, P. Gagnon, P. Kurup, C. Murphy, V. Ramasamy, J. Robins, J. Zuboy, D. Oladosu, J. Hoffmann, 2022 Annual Technology Baseline (ATB) Cost and Performance Data for Electricity Generation Technologies, Tech. Rep. 5716, DOE Open Energy Data Initiative (OEDI); National Renewable Energy Laboratory (NREL) (Jun. 2022). doi:10.25984/1871952.
URL https://www.osti.gov/dataexplorer/biblio/dataset/1871952

[26] R. Lueken, J. Apt, The effects of bulk electricity storage on the PJM market, Energy Systems 5 (4) (2014) 677–704. doi:10.1007/s12667-014-0123-7.
URL https://doi.org/10.1007/s12667-014-0123-7

[27] M. Bruchon, Z. L. Chen, J. Michalek, Cleaning up while Changing Gears: The Role of Battery Design, Fossil Fuel Power Plants, and Vehicle Policy for Reducing Emissions in the Transition to Electric Vehicles, Environmental Science & TechnologyPublisher: American Chemical Society (Feb. 2024). doi:10.1021/acs.est.3c07098.
URL https://doi.org/10.1021/acs.est.3c07098

[28] A. Weis, P. Jaramillo, J. Michalek, Consequential life cycle air emissions externalities for plug-in electric vehicles in the PJM interconnection, Environmental Research Letters 11 (2) (2016) 024009, publisher: IOP Publishing. doi:10.1088/1748-9326/11/2/024009.
URL https://dx.doi.org/10.1088/1748-9326/11/2/024009

[29] B. Sergi, W. Cole, Operating Reserves in ReEDS, Tech. Rep. NREL/PR-6A40-81706, National Renewable Energy Lab. (NREL), Golden, CO (United States) (Dec. 2021). doi:10.2172/1841961.
URL https://www.osti.gov/biblio/1841961

[30] M. T. Craig, P. Jaramillo, H. Zhai, K. Klima, The Economic Merits of Flexible Carbon Capture and Sequestration as a Compliance Strategy with the Clean Power Plan, Environmental Science & Technology 51 (3) (2017) 1102–1109, publisher: American Chemical Society. doi:10.1021/acs.est.6b03652.
URL https://doi.org/10.1021/acs.est.6b03652

[31] EPA Report on the Social Cost of Greenhouse Gases: Estimates Incorporating Recent Scientific Advances, Tech. rep. (Nov. 2023).